CHAPTER TWO

DISCOVERY OF HIGHLY SELECTIVE, SALEN-SUPPORTED COBALT CATALYSTS FOR PROPYLENE OXIDE/CO_2 COPOLYMERIZATION

Reprinted in part with permission from the

Journal of the American Chemical Society, **2005**, 127, 10869 – 10878.

Journal of Polymer Science, Polymer Chemistry, **2006**, *In Press.*

2.1 Introduction

CO_2 is an ideal synthetic feedstock because it is abundant, inexpensive, and nontoxic. Considerable interest in CO_2 activation with transition metal complexes is directed toward its use in organic synthesis.[1] One growing area in CO_2 chemistry is the development of catalysts for the alternating copolymerization of CO_2 and epoxides to form polycarbonates,[2] a field pioneered by Inoue and coworkers in the late 1960s.[3]

The copolymerization of CO_2 and alicyclic epoxides with discrete metal complexes has been well documented.[2] Aliphatic epoxides, such as propylene oxide (PO), remain a greater challenge owing to the concomitant production of propylene carbonate (PC) as shown in Scheme 2.1.[4-12] The generalized sequence for PO/CO_2 copolymerization involves epoxide ring opening by a metal carbonate to give a metal alkoxide, followed by CO_2 insertion (Scheme 2.2). In addition, PC can be formed through a back-biting reaction from the propagating alkoxide.[5]

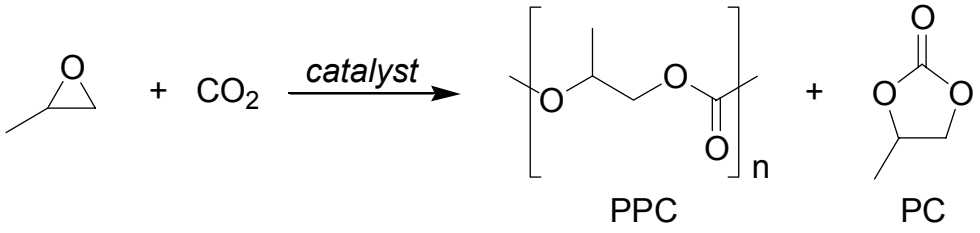

Scheme 2.1. Reaction of PO and CO_2 to yield PPC and PC.

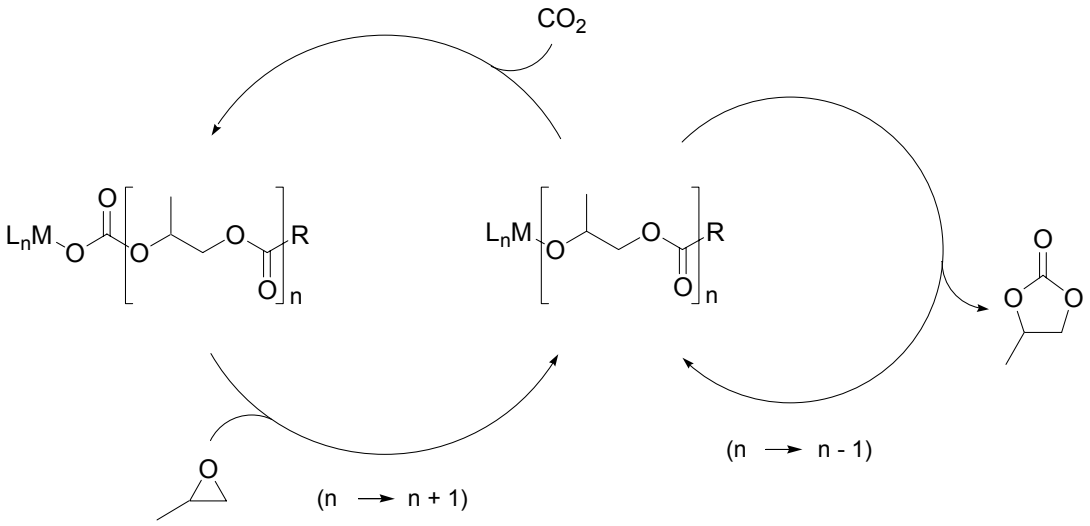

Scheme 2.2. Copolymerization of PO and CO_2 using discrete metal alkoxides (R = OR') and carboxylates (R = Alkyl, Aryl).

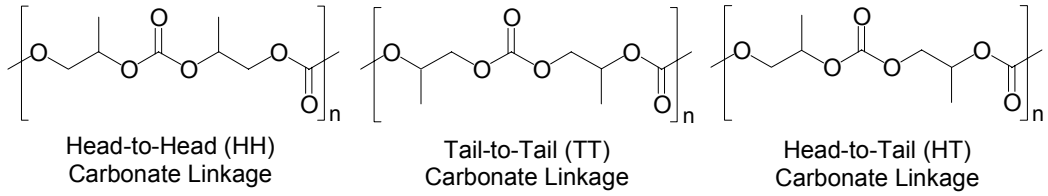

Figure 2.1. Regiochemistry of PPC.

The ring opening of PO can occur at the methylene carbon (α attack) with retention of stereochemistry or at the methine (β attack) carbon with retention or inversion of stereochemistry.[13] If the nature of the PO ring opening is consistent throughout the copolymerization (α or β), regioregular poly(propylene carbonate) (PPC) with a high % head-to-tail (HT) connectivity is observed (Figure 2.1). Furthermore, regioregular PPC can be highly stereoregular with the same (isotactic) or

alternating (syndiotactic) relative stereocenters in the polymer chain. Alternatively, a moderately stereoregular PPC may consist of either alternating meso (*m*) and racemo (*r*) diads (heterotactic) or the same relative stereocenter at every other pendant methyl (hemiisotactic). Finally, regioregular atactic PPC has little or no stereoregularity (Figure 2.2).

A catalyst with a preference for PO ring opening at one carbon (α or β) and for one or alternating enatiomers ((*S*) or (*R*)) of *rac*-PO can be applied to achieve regio- and/or stereoregular PPC (enantiomorphic-site control). Alternatively, the stereogenic center from the last enchained PO can influence the stereochemistry of the next PO enchainment which can also lead to regio- and/or stereoregular PPC (chain-end control) (Scheme 2.3).[14]

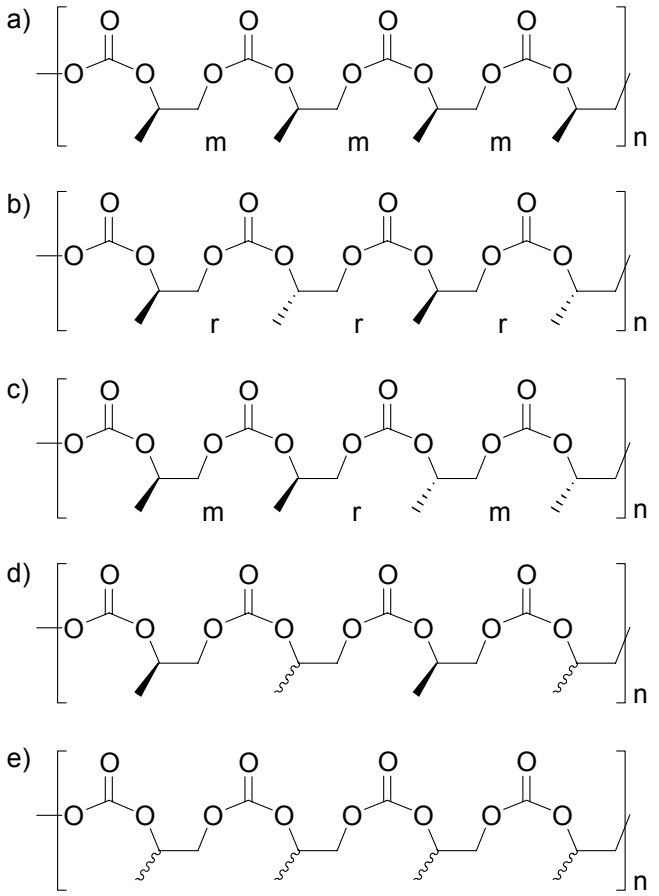

Figure 2.2. Regioregular PPC in order of decreasing stereoregularity. a) isotactic, b) syndiotactic, c) heterotactic, d) hemiisotactic, e) atactic (m = *meso* diad, r = *racem*o diad).

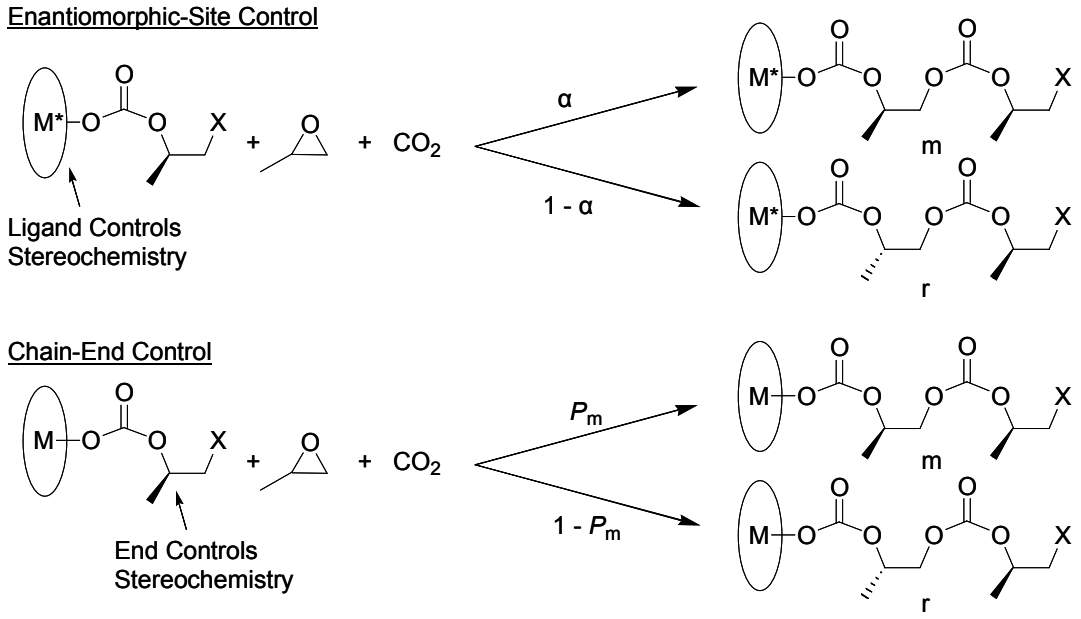

Scheme 2.3. Enantiomorphic-site and chain-end control mechanisms for PPC stereocontrol (α is the enantioface selectivity of the enantiomorphic site, P_m is the probability of a *meso* diad).

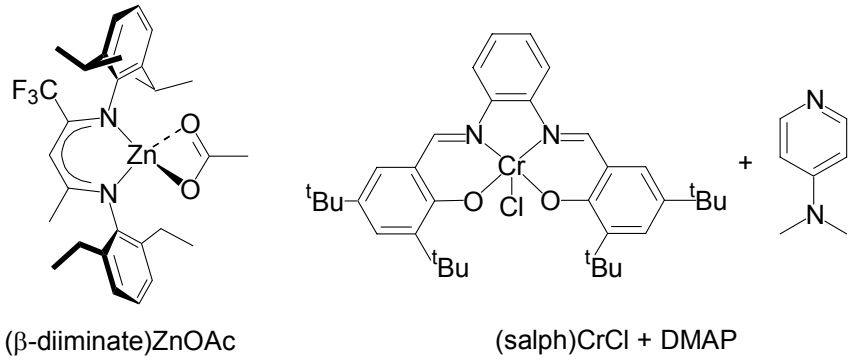

Figure 2.3. Catalysts for the copolymerization of PO and CO_2 (salph = *N*,*N*'-bis(salicylidene)phenylenediamine, DMAP = 4-dimethylaminopyridine).

In an effort to achieve PPCs with high activity and control of polymer microstructure, recent work has focused on single-site catalysts of the general formula L_nM (L_n = organic ligand, M = metal). Notably, these discrete polymerization catalysts can be designed at the molecular level, providing for a tunable active site. Advances using *β*-diiminate zinc or salen-type (salen = *N,N′*-bis(salicylidene)-1,2-diaminoalkane) chromium catalysts with Lewis base or organic-based, ionic cocatalysts (Figure 2.3) have resulted in the highest reported activities for this reaction but produce significant quantities of the byproduct PC[4-6, 9, 11, 12] and/or exhibit little control of PPC microstructure.[2] In an effort to improve selectivity for PPC over PC as well as to generate PPC with controlled architectures, we searched for metal/ligand combinations known to effect stereo- and regioselective reactions with PO. Jacobsen and coworkers have reported chiral (salen)Co^{III} carboxylates for the hydrolytic kinetic resolution of epoxides with remarkable efficiencies.[15] When we applied (*R,R*)-(salen-**1**)CoOAc (**2.1**, Figure 2.4) to *rac*-PO/CO_2 copolymerization, we observed unprecedented selectivity for highly regioregular PPC.[16] Specifically, catalyst **2.1** generated PPC with 99% carbonate linkages (Figure 2.5) and 93% HT connectivity (Figure 2.6); however, it did not yield high number average molecular weights (M_n)s, narrow molecular weight distributions (MWD)s, or fast reaction rates characteristic of the zinc- and chromium-based alternatives.[4-6, 9, 11, 12]

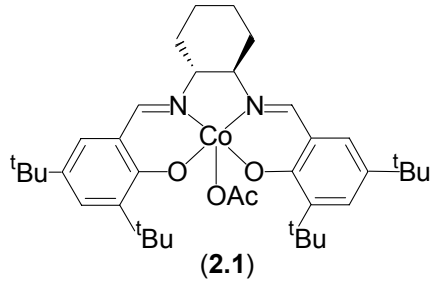

(**2.1**)

Figure 2.4. Catalyst **2.1** for the copolymerization of PO and CO_2.

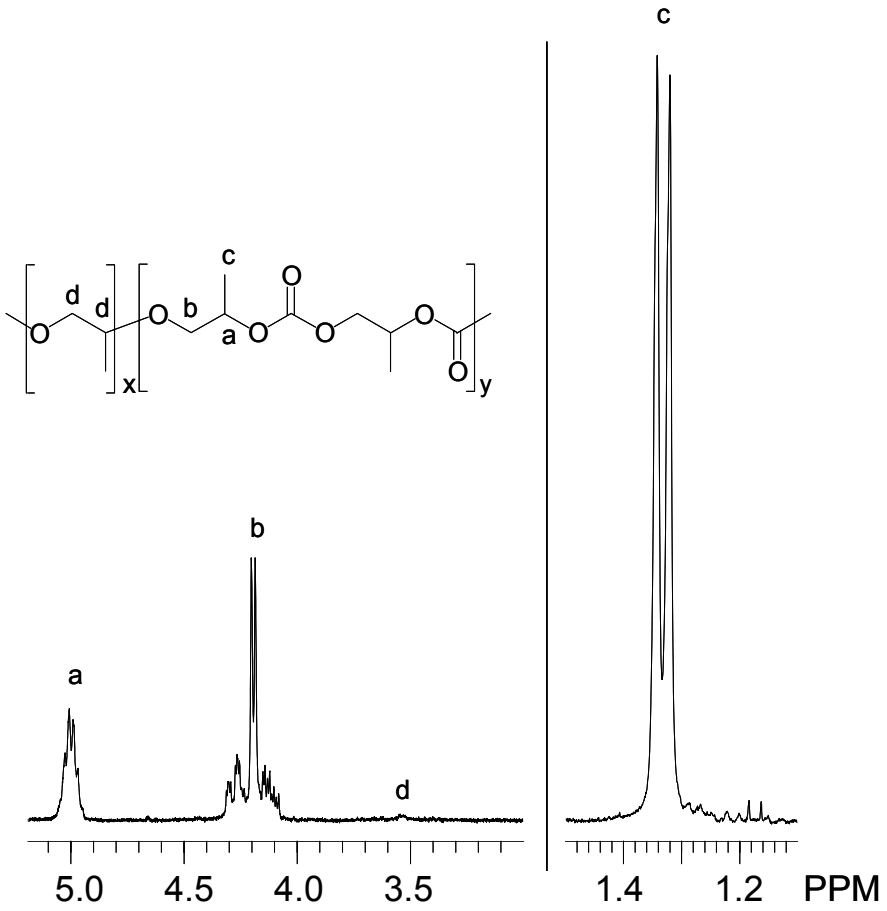

Figure 2.5. ^{1}H NMR spectrum ($CDCl_3$, 300 MHz) of regioregular PPC as generated by catalyst **2.1** and *rac*-PO/CO_2.

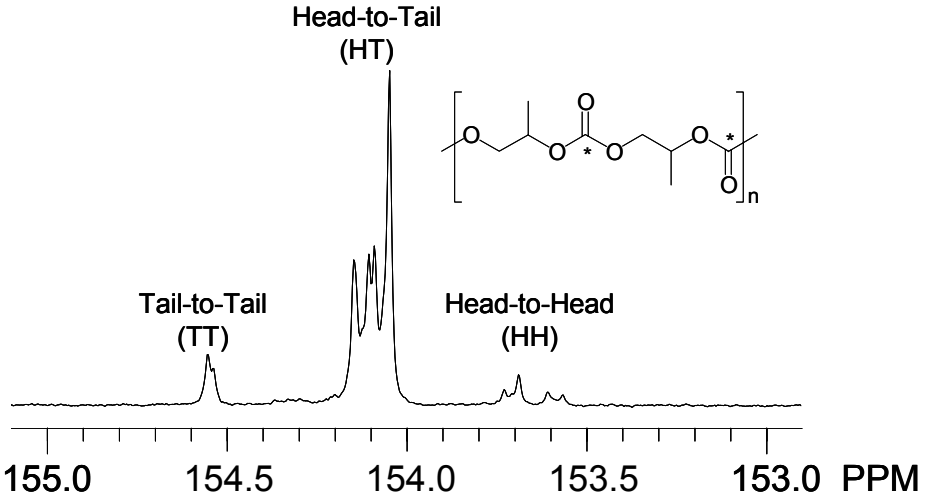

Figure 2.6. Carbonyl region of the quantitative $^{13}C\{^1H\}$ NMR spectrum ($CDCl_3$, 125 MHz, d_1 = 10s) of regioregular PPC as generated by catalyst **2.1** and *rac*-PO/CO_2.

Herein, we present our continued studies concerning PO/CO_2 copolymerization using (salen)CoX (X = halide or carboxylate) complexes. We explore the influence of the reaction conditions, catalyst axial ligand/initiator (X) and salen-ligand structure on catalyst activity, product selectivity, stereo-, and regioselectivity. Additionally, we describe the diverse PPC stereo- and regiochemistries that result from variation of the relative catalyst and PO stereochemistry. Once optimized, these systems demonstrate unprecedented selectivities for PPC over PC while accessing isotactic, syndiotactic, atactic, regioregular, and regioirregular PPCs with narrow MWDs.

2.2 Development of a highly selective catalyst for regioregular PPC

2.2.1 Initial discovery

We recently reported that complex **2.1** catalyzes the alternating copolymerization of *rac*- or (*S*)-PO and CO_2 with unprecedented selectivity for PPC

over PC. Average turnover frequencies (TOF)s, however, were limited to less than 85 turnovers per hour.[16] In addition, the MWDs of PPC synthesized by complex **2.1** are relatively broad (MWD = 1.2 – 2.6), and the measured M_n values of the polymers are lower than the corresponding theoretical values. As it had been shown that minor alterations in synthetic conditions and ligand structure can result in large differences in the catalytic performance of salen-type chromium complexes for epoxide/CO_2 copolymerization,[6, 11, 17, 18] we proceeded to explore (salen)CoX complexes for PO/CO_2 copolymerization with a focus on optimizing reaction conditions and catalyst structure in an effort to improve molecular weight control, increase polymerization activity, and obtain mechanistic insight.

2.2.2 Synthesis of PPC with a narrow MWD

We initially observed that PPCs synthesized by catalyst **2.1** under ambient reaction conditions show bimodal gel permeation chromatographs (GPC)s with broad MWDs. We speculated this was due to chain transfer to trace water present in the copolymerization, a pathway similar to that reported by Inoue and coworkers for ethylene oxide polymerization with aluminum porphyrin catalysts.[19] As the propagating species is presumably an alkoxide bound to cobalt (CoOP^1-OAc; P^1 = PPC), the growing polymer can be displaced from the catalyst by water resulting in an alcohol terminated polymer (AcO-P^{1}OH). The resultant intermediate complex, (*R,R*)-(salen-**1**)CoOH, can initiate an additional polymer chain (P^2; P^2 = PPC) to form (*R,R*)-(salen-**1**)CoOP^{2}OH. The original alcohol terminated polymer, AcO-P^{1}OH, can also undergo chain transfer reactions, generating the species (*R,R*)-(salen-**1**)CoOP^1-OAc and displacing HO-P^{2}OH. Notably, if the rate of exchange is rapid compared to the rate of propagation, polymer HO-P^{2}OH can propagate on either –OH end, whereas the AcO-P^{1}OH species can only propagate from one end. Once the polymerization reaction is quenched, the M_n value of HO-P^{2}OH is expected to be at least two times

that of AcO-P[1]OH (Scheme 2.4). To support this assessment, we carried out the copolymerization using catalyst (*R,R*)-(salen-**1**)CoI (**2.2**), where the catalyst axial ligand/initiator is UV active. Furthermore, we expected to observe the low M_n PPC component (I-P[1]OH) with both the refractive index (RI) and ultraviolet (UV) GPC detectors, whereas the UV-silent high M_n PPC component (HO-P[2]OH) would only be seen with the RI detector. This was indeed the case, where the **2.2** catalyzed PO/CO_2 copolymerization under ambient reaction conditions yielded PPC with a M_n = 15.9 kg/mol that showed no UV-activity, and PPC with a M_n = 5.7 kg/mol that was UV-active (Figure 2.7).

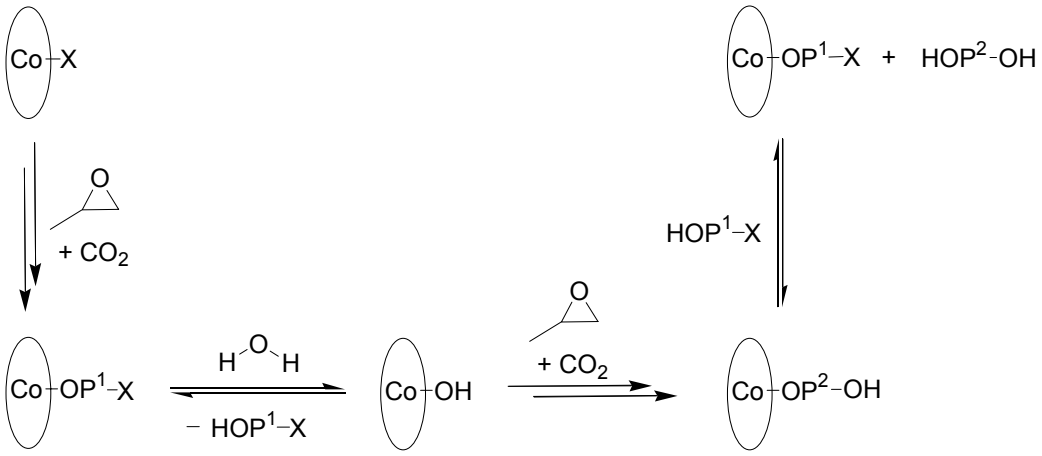

Scheme 2.4. Exchange of propagating species and water using cobalt-salen catalysts (P^1, P^2 = PPC, X = halide or carboxylate).

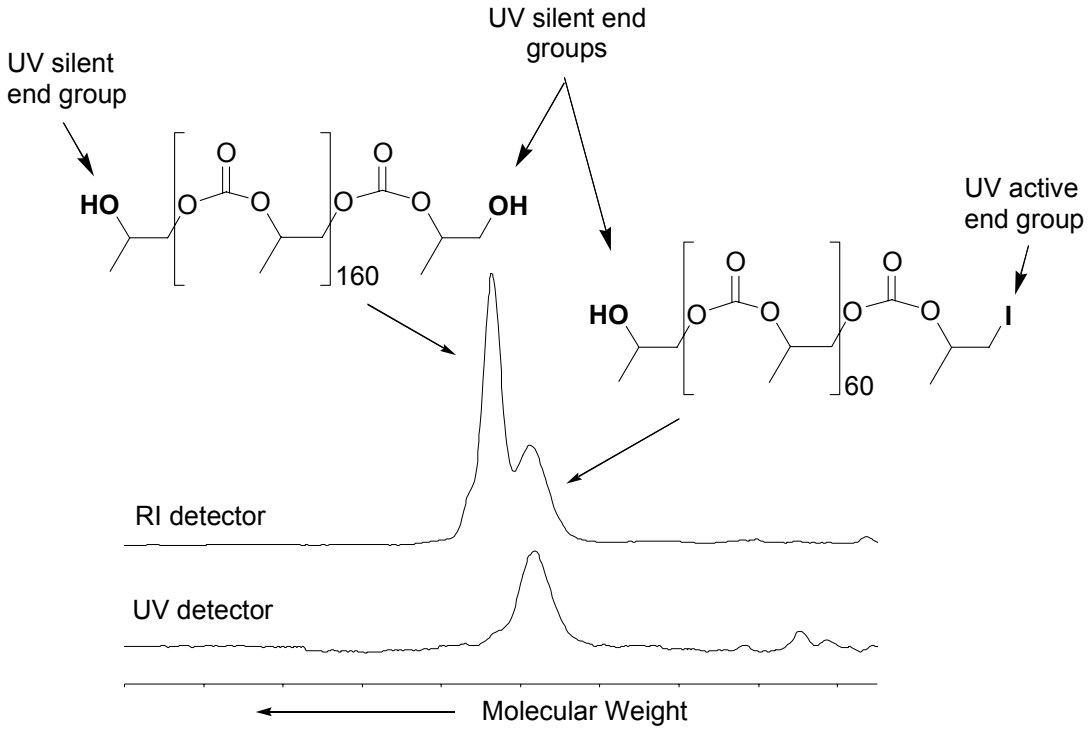

Figure 2.7. GPC (relative to polystyrene standards) of PPC generated using catalyst (*R,R*)-(salen-**1**)CoI (**2.2**) under ambient reaction conditions.

Table 2.1 compares the *rac*-PO/CO_2 copolymerizations carried out under air-free (entries 1 and 3) and ambient (entries 2 and 4) conditions using catalysts **2.1** and **2.2**. The PPC generated under air-free conditions exhibits a measured M_n that agrees more closely with the theoretical value and has a MWD less than 1.2. In all cases, PPC with ≥96% carbonate linkages and ≥79% HT connectivity was achieved with no detectable PC. Although the removal of trace water provides for a narrow MWD, it is not a necessary condition for the generation of PPC.

Table 2.1. Effect of ambient and air-free reaction conditions: (*R,R*)-(salen-**1**)CoX (X = OAc (**2.1**), I (**2.2**)) catalyzed copolymerization of *rac*-PO/CO_2.[a]

Entry	Complex	Reaction Conditions	Time (h)	PPC Yield[b] (%)	TOF[c] (h^{-1})	Theoretical M_n[d] (kg/mol)	M_n[e] (kg/mol)	M_w/M_n[e]	Head-to-Tail Linkages[f] (%)
1	**2.1**	air-free	2	30	74	15.1	15.5	1.16	83
2	**2.1**	ambient	2	25	62	12.7	10.4[g]	1.31	83
3	**2.2**	air-free	5	44	43	21.9	19.6	1.15	79
4	**2.2**	ambient	5	36	37	18.9	9.5[g]	1.33	81

[a] Copolymerizations run neat with [*rac*-PO]:[Co] = 500:1 at 22 °C with 800 psi of CO_2. Selectivity for PPC over PC was > 99% in all cases. PPC contains ≥ 96% carbonate linkages as determined by ^{1}H NMR spectroscopy ($CDCl_3$, 300 MHz). [b] Based on isolated PPC yield. [c] Turnover frequency for PPC = (mol PO/(mol Co · h)). [d] Calculated M_n = TOF · time · 102 kg/mol. [e] Determined by GPC, calibrated with polystyrene standards in THF at 40 °C. [f] Determined by quantitative $^{13}C\{^1H\}$ NMR spectroscopy ($CDCl_3$, 125 MHz, d_1 = 10s). [g] M_n averaged over a bimodal GPC distribution.

2.2.3 Catalyst axial ligand/initiator (X)

Jacobsen and coworkers have conducted extensive studies that support a bimetallic mechanism for the chiral (salen-**1**)CoX (X = nucleophile or counterion) catalyzed kinetic resolution of terminal epoxides (Scheme 2.5).[20] With these systems, they observed a large reaction rate dependence on the composition of the axial ligand/counterion of the catalyst (X). These results led us to suspect that the nature of the axial ligand would likewise influence the rate of our PO/CO_2 copolymerizations. The polymerization data of complexes (*R,R*)-(salen-**1**)CoX with X = OAc (**2.1**), I (**2.2**), pentafluorobenzoate ($OBzF_5$) (**2.3**), Cl (**2.4**), and Br (**2.5**), are collected in Table 2.2. Although the behavior of catalysts **2.1** and **2.3** proved largely similar (Table 2.2, entries 1 and 3), use of the various halides **2.2**, **2.4**, or **2.5**, resulted in substantial changes in catalytic activity (entries 2, 4 and 5). The order of increasing activity for copolymerization with (*R,R*)-(salen-**1**)CoX complexes is X = I < Cl < OAc ≈ $OBzF_5$ < Br, with the most active catalyst, **2.5**, producing PPC with a TOF of 89 h^{-1} (entry 4). Despite activity differences, all systems yielded atactic PPC with ≥92% carbonate linkages, ≥82% HT connectivity, narrow MWDs, and no detectable PC.

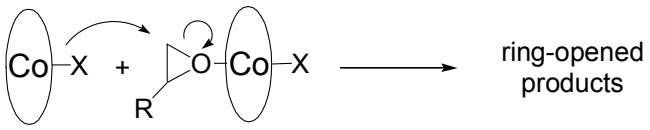

Scheme 2.5. Bimetallic (salen)CoX (X = nucleophile) ring opening of epoxides proposed by Jacobsen and coworkers.

Table 2.2. Effect of initiating group: (*R,R*)-(salen-**1**)CoX (X = OAc (**2.1**), I (**2.2**), $OBzF_5$ (**2.3**), Cl (**2.4**), Br (**2.5**)) catalyzed *rac*-PO/CO_2 copolymerization.[a]

Entry	Complex	PPC Yield[b] (%)	TOF[c] (h^{-1})	M_n[d] (kg/mol)	M_w/M_n[d]	Head-to-Tail Linkages[e] (%)
1	**2.1**	30	74	15.5	1.16	83
2	**2.2**	13	32	10.4	1.17	85
3	**2.3**	32	78	14.1	1.22	82
4	**2.4**	26	64	13.4	1.19	82
5	**2.5**	36	89	21.0	1.14	82
6	**2.2** + **2.5** (50:1)	28	69	16.2	1.24	81

[a] Copolymerizations run neat with [*rac*-PO]:[Co] = 500:1 at 22 °C with 800 psi of CO_2 for 2 h. Selectivity for PPC over PC was > 99% in all cases. All product PPC contains ≥ 92% carbonate linkages as determined by ^{1}H NMR spectroscopy ($CDCl_3$, 300 MHz). [b] Based on isolated PPC yield. [c] Turnover frequency for PPC = (mol PO/(mol Co · h)). [d] Determined by GPC calibrated with polystyrene standards in THF at 40 °C. [e] Determined by quantitative $^{13}C\{^1H\}$ NMR spectroscopy ($CDCl_3$, 125 MHz, d_1 = 10s).

Because the copolymerization rate exhibits a pronounced dependence on the nature of the axial ligand (X), we speculated that a bimetallic initiation similar to that proposed by Jacobsen and coworkers was operable. As such, we anticipated that through combining the slowest catalyst, **2.2**, with the more active **2.5**, its copolymerization activity would improve. This prediction was indeed correct: as little as 2% of **2.5** with catalyst **2.2** achieved a TOF of 69 h^{-1} while maintaining an overall [PO]:[Co] loading of 500:1 (Table 2.2, entry 6). This copolymerization rate is more than double that of the unassisted **2.2** catalyzed reaction, even though $[I^-][Br^-]$ is 50:1. PPC produced with the mixed catalyst system maintains 92% carbonate linkages and 81% HT connectivity although there is slight MWD broadening.

2.2.4 Crystal structure of catalyst 2.4

Although the majority of the (*R,R*)-(salen-**1**)CoX (X = halide or carboxylate) complexes were obtained as powders, X-ray quality crystals of catalyst **2.4** were obtained from slow evaporation of benzene-d_6. The X-ray crystal structure of **2.4** with selected bond angles and bond lengths is shown in Figure 2.8. Complex **2.4** is pseudo square-pyramidal with the cobalt located slightly above the plane of the salen ligand in the direction of the axial ligand.

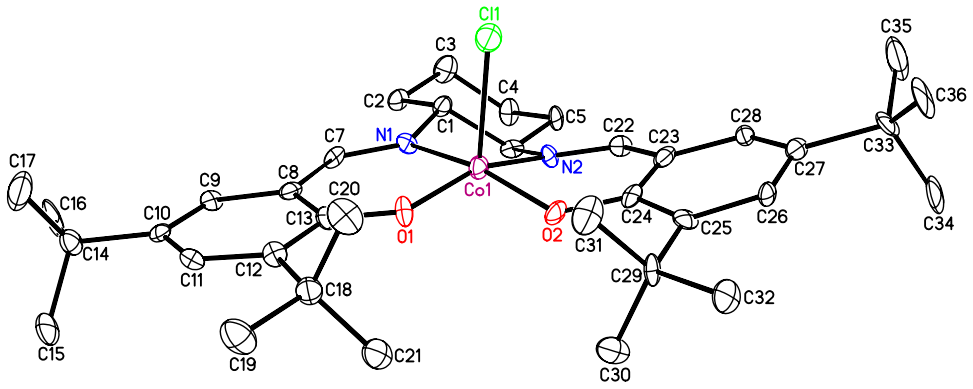

Figure 2.8. ORTEP drawing of (*R,R*)-(salen-**1**)CoCl (**2.4**) (non-hydrogen atoms) with thermal ellipsoids drawn at the 40% probability level. Selected bond lengths (Å) and angles (°): Co(1)-Cl(1) 2.330(2), Co(1)-O(1) 1.845(5), Co(1)-O(2) 1.844(5), Co(1)-N(1) 1.882(6), Co(1)-N(2) 1.887(6), O(1)-Co(1)-Cl(1) 102.7(2), O(2)-Co(1)-Cl(1) 98.3(2), N(1)-Co(1)-Cl(1) 93.9(2), N(2)-Co(1)-Cl(1) 95.6(2).

2.2.5 Salen ligand structure

While using the axial ligand X = Br that provided for the most active catalyst, we proceeded to investigate the influence of the salen ligand structure on *rac*-PO/CO_2 copolymerization activity using eleven different (salen)CoBr catalysts. Specifically, six (salen-**1** – salen-**6**) were chosen to investigate the effects of variation in the diimine

backbone while the remainder (salen-**7** – salen-**11**) encompass steric and electronic modifications to the phenolate *ortho* and *para* positions (Figure 2.9).

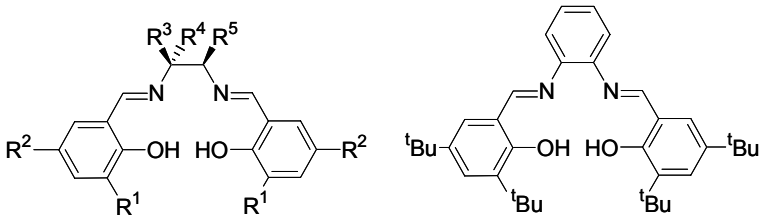

Ligand		R^1	R^2	R^3	R^4	R^5
(*R,R*)-(salen-**1**)H_2	(**2.6**)	^{t}Bu	^{t}Bu	H	*trans* -(*R,R*)-$(CH_2)_4$-	
rac-(salen-**1**)H_2	(**2.7**)	^{t}Bu	^{t}Bu	H	*trans* -(*R,R*)-$(CH_2)_4$-	
(*R*)-(salen-**2**)H_2	(**2.8**)	^{t}Bu	^{t}Bu	(*R*)-Me	H	H
(salen-**3**)H_2	(**2.9**)	^{t}Bu	^{t}Bu	H	H	H
(salen-**4**)H_2	(**2.10**)	^{t}Bu	^{t}Bu	Me	Me	H
(*R,R*)-(salen-**5**)H_2	(**2.11**)	^{t}Bu	^{t}Bu	H	(*R*)-Ph	*trans*-(*R*)-Ph
(*R,R*)-(salen-**7**)H_2	(**2.13**)	^{t}Bu	H	H	*trans* -(*R,R*)-$(CH_2)_4$-	
(*R,R*)-(salen-**8**)H_2	(**2.14**)	^{t}Bu	Br	H	*trans* -(*R,R*)-$(CH_2)_4$-	
(*R,R*)-(salen-**9**)H_2	(**2.15**)	H	^{t}Bu	H	*trans* -(*R,R*)-$(CH_2)_4$-	
(*R,R*)-(salen-**10**)H_2	(**2.16**)	Me	H	H	*trans* -(*R,R*)-$(CH_2)_4$-	
(*R,R*)-(salen-**11**)H_2	(**2.17**)	cumyl	cumyl	H	*trans* -(*R,R*)-$(CH_2)_4$-	

Figure 2.9. Salen ligands used to synthesize (salen)CoBr PO/CO_2 copolymerization catalysts. Cumyl = α,α'-dimethylbenzyl.

Table 2.3 shows the effects of salen ligand structure on catalyst activity and regioselectivity. Catalyst **2.5** has a TOF of 63 h^{-1} for the *rac*-PO/CO_2 copolymerization, yielding PPC with 81% HT connectivity (Table 2.3, entry 1). Comparable to this are catalysts (*R*)-(salen-**2**)CoBr (**2.18**) and (salen-**4**)CoBr (**2.19**) (entries 2 and 4), indicating that a chiral ligand is not necessary for high activity and

regioselectivity. It is essential, however, to employ a substituted diimine backbone, as the unsubstituted complex (salen-**3**)CoBr (**2.20**) was totally inactive (entry 3). We suspect that complex **2.20** is relatively unstable under the reaction conditions employed, undergoing reduction in situ to form the inactive cobalt (II) complex (salen-**3**)Co^{II} (**2.21**).[a] Compared to catalyst **2.5**, both (*R,R*)-(salen-**5**)CoBr (**2.22**) and (salen-**6**)CoBr (**2.23**) were less active for *rac*-PO/CO_2 copolymerization with reduced regioselectivity in the PPC formed (entries 5 and 6). In addition, the PPC generated using catalyst **2.23** has only 89% carbonate linkages, suggesting that PO and CO_2 insertion into the propagating alkoxide are competitive in this case. Notably, the phenyl substituted diimine backbones are detrimental to catalyst solubility. In general, we have shown that salen ligands with alkylated diimine backbones are most beneficial for high activity and regioselectivity, although the specific choice of alkyl substituents has only a minimal impact on catalyst performance.

Using the cyclohexyl diimine ligand backbone, we investigated the influence of the phenolate *ortho* and *para* substituents on the (salen)CoBr catalyzed *rac*-PO/CO_2 copolymerization. Catalysts (*R,R*)-(salen-**7**)CoBr (**2.24**) and (*R,R*)-(salen-**8**)CoBr (**2.25**) produce PPC with comparable activity to catalyst **2.5**, although the product polymer is less regioregular (Table 1.2, entries 7 and 8). Additionally, the PPC generated using catalyst **2.25** has a M_n value substantially greater than that of the calculated value. The may be the result of a fraction of the **2.25** catalyst undergoing reduction in situ to the inactive (*R,R*)-(salen-**8**)Co^{II} (**2.26**) prior to initiation. Using catalyst (*R,R*)-(salen-**9**)CoBr (**2.27**), no PPC was formed, which we again attribute to the instability of this complex under the reaction conditions employed (entry 9).

[a] When the *rac*-PO/CO_2 copolymerization is carried out at low CO_2 pressures (<100 psi) in a Fischer-Porter bottle, the reduction of (salen)Co^{III} to (salen)Co^{II} can be observed as a red solid precipitating from the reaction. This reaction is also thought to occur at higher CO_2 pressures, however the CO_2 must be vented from the Parr reactor before the reaction mixture can be seen, preventing direct observation.

Decreasing or increasing the steric bulk of the phenolate ((*R,R*)-(salen-**10**)CoBr (**2.28**), (*R,R*)-(salen-**11**)CoBr (**2.29**)) reduces catalyst activity as compared to **2.5** (entries 10 and 11). Furthermore, the PPC generated using **2.28** has only 69% carbonate linkages, suggesting that the reduced steric bulk of the catalyst is detrimental for high carbonate incorporation. The more bulky **2.29** is the most regioselective catalyst we report. Overall, the most active and regioselective *rac*-PO/CO_2 copolymerization catalyst contains a salen ligand with an alkylated diimine backbone, and *tert*-butyl substituents in the *ortho* and *para* positions of the phenolate.

Table 2.3. Effect of catalyst structure: (salen)CoBr catalyzed *rac*-PO/CO_2 copolymerization.[a]

Entry	Catalyst		PPC Yield[b] (%)	TOF[c] (h^{-1})	Carbonate Linkages[d] (%)	M_n[e] (kg/mol)	M_w/M_n[e]	Head-to-Tail Connectivity[f] (%)
1	(*R,R*)-(salen-**1**)CoBr	(**2.5**)	38	63	97	20.2	1.15	81
2	(*R*)-(salen-**2**)CoBr	(**2.18**)	32	53	97	13.9	1.18	82
3[g]	(salen-**3**)CoBr	(**2.20**)	0	0	NA	NA	NA	NA
4	(salen-**4**)CoBr	(**2.19**)	38	63	>99	21.1	1.16	85
5	(*R,R*)-(salen-**5**)CoBr	(**2.22**)	12	20	99	10.1	1.14	76
6	(salen-**6**)CoBr	(**2.23**)	14	23	89	11.3	1.29	79
7	(*R,R*)-(salen-**7**)CoBr	(**2.24**)	33	55	96	15.2	1.13	76
8	(*R,R*)-(salen-**8**)CoBr	(**2.25**)	43	72	94	35.8	1.15	70
9[g]	(*R,R*)-(salen-**9**)CoBr	(**2.27**)	0	0	NA	NA	NA	NA
10	(*R,R*)-(salen-**10**)CoBr	(**2.28**)	8	13	69	4.5	1.12	80
11	(*R,R*)-(salen-**11**)CoBr	(**2.29**)	11	18	>99	9.1	1.13	89

[a] Copolymerizations run neat with [*rac*-PO]:[Co] = 500:1 at 22 °C with 800 psi of CO_2 for 3 h. Selectivity for PPC over PC was > 99:1 for entries 1 – 10, and 97:3 for entry 11. [b] Based on isolated PPC yield. [c] Turnover frequency for PPC = (mol PO/(mol Co · h)). [d] Determined by ^{1}H NMR spectroscopy ($CDCl_3$, 300 MHz). [e] Determined by GPC calibrated with polystyrene standards in THF at 40 °C. [f] Determined by quantitative $^{13}C\{^1H\}$ NMR spectroscopy ($CDCl_3$, 125 MHz, d_1 = 10s). [g] Copolymerization run for 6 h.

2.3 Synthesis of stereo- and regioregular PPC

We previously reported that catalyst **2.1** preferentially enchains (*S*)- over (*R*)-PO (k_{rel} = 2.8) in the *rac*-PO/CO_2 copolymerization.[16] Also, substitution of (*S*)- for *rac*-PO increases the HT connectivity of the product PPC from 80% to 93%. These initial experiments indicate that the chiralities of the monomer and the catalyst strongly influence the polymerization activities and the product PPC regiochemistry. Furthermore, the relationship among the catalyst and PO stereochemistry and the resultant PPC microstructure provides mechanistic insight. As such, we were eager to pursue this topic with one of the more active catalysts, **2.5**.

Table 2.4 lists the copolymerization data for **2.5** and *rac*-(salen-**1**)CoBr (**2.30**) with *rac*-, (*S*)-, and (*R*)-PO/CO_2. As stated above, the copolymerization of *rac*-PO and CO_2 with catalyst **2.5** produces atactic PPC with 82% HT connectivity (Table 2.4, entry 1; Figure 2.10a; Scheme 2.6a). Under the same reaction conditions, but replacing *rac*- with (*S*)-PO, the catalytic activity increases from 89 to 120 turnovers per hour, and the resultant PPC is isotactic with 93% HT connectivity (Table 2.4, entry 2; Figure 2.10b; Scheme 2.6b). This result is consistent with our earlier work[16] and indicates that the (*R,R*)- catalyst makes fewer regioerrors when only (*S*)-PO is present. Degradation of this polymer to PC while conserving all stereocenters[10] yielded a (*S*)-PC:(*R*)-PC ratio of 97:3 as determined by gas chromatography (GC). The high (*S*)-content of the PPC suggests that transcarbonation and PC reinsertion mechanisms do not readily occur, and that the PO ring opening process predominately takes place at the methylene or methine carbon with stereochemical retention. Furthermore, when the **2.5** catalyzed (*S*)-PO/CO_2 copolymerization is carried out in the presence of *rac*-PC, the PPC formed is highly isotactic, implicating that PC reinsertion mechanisms do not occur. Chisholm and coworkers have previously shown the possibility of PO ring opening at the methine carbon with stereochemical retention in related chromium and

aluminum catalyst systems.[13] Although a consistent methine (*S*)-PO ring opening process with stereochemical retention would result in PPC with a high (*S*)-content, we put forth that the preferred reaction pathway in our systems is the sterically favored attack at the methylene carbon.

Table 2.4. (*R,R*)-(Salen-**1**)CoBr (**2.5**) and *rac*-(salen-**1)**CoBr (**2.30**) catalyzed PO/CO_2 copolymerization using *rac*-, (*S*)-, and (*R*)-PO.[a]

Entry	Catalyst	Epoxide	PPC Yield[b] (%)	TOF[c] (h^{-1})	M_n[d] (kg/mol)	M_w/M_n[d]	Head-to-Tail Linkages[e] (%)
1	**2.5**	*rac*-PO	36	89	21.0	1.14	82
2	**2.5**	(*S*)-PO	49	120	20.1	1.21	93
3	**2.5**	(*R*)-PO	20	50	13.3	1.16	43
4	**2.30**	(*R*)-PO	42	100	26.9	1.16	83
5	**2.30**	*rac*-PO	41	100	21.8	1.22	84

[a] Copolymerizations run neat with [PO]:[Co] = 500:1 at 22 °C with 800 psi of CO_2 for 2 h. Selectivity for PPC over PC was > 99% in all cases. All product PPC contains ≥ 92% carbonate linkages as determined by ^{1}H NMR spectroscopy ($CDCl_3$, 300 MHz). [b] Based on isolated PPC yield. [c] Turnover frequency for PPC = (mol PO/(mol Co · h)). [d] Determined by GPC calibrated with polystyrene standards in THF at 40 °C. [e] Determined by quantitative $^{13}C\{^1H\}$ NMR spectroscopy ($CDCl_3$, 125 MHz, d_1 = 10s).

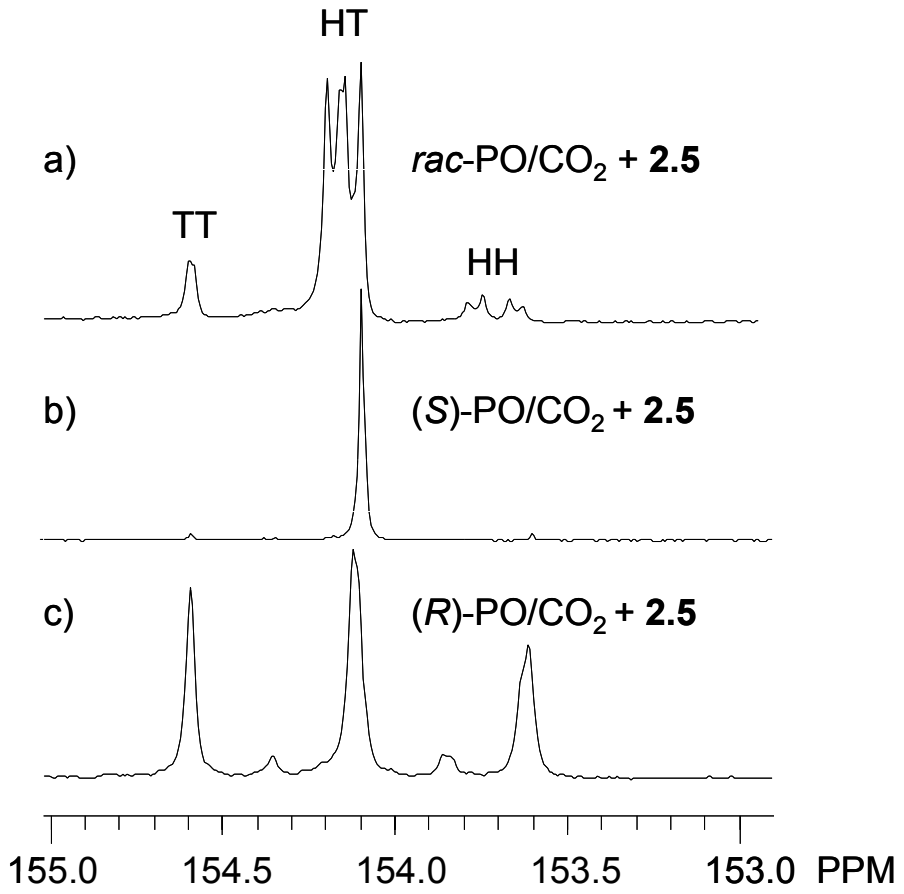

Figure 2.10. Carbonyl region of the quantitative $^{13}C\{^1H\}$ NMR ($CDCl_3$, 125 MHz, d_1 = 10s) spectra of PPC synthesized from (a) (*R,R*)-(salen-**1**)CoBr (**2.5**) and *rac*-PO/CO_2, (b) **2.5** and (*S*)-PO/CO_2, and (c) **2.5** and (*R*)-PO/CO_2.

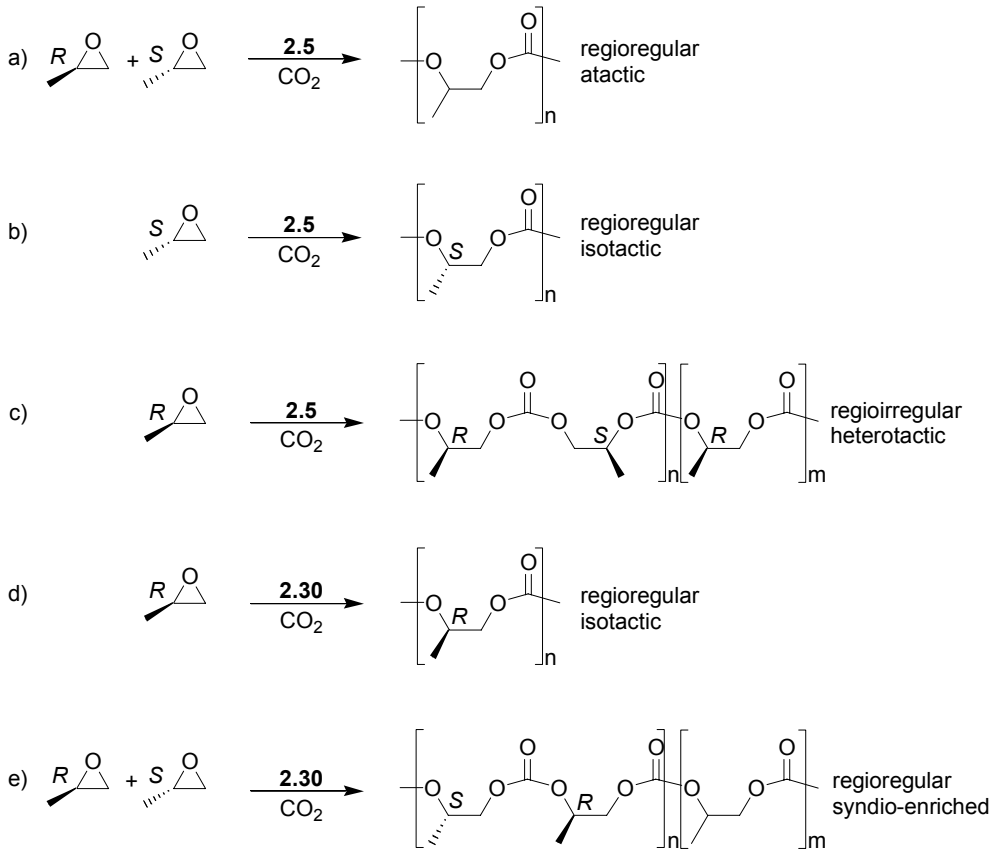

Scheme 2.6. PO/CO_2 copolymerization using (a) *rac*-PO/CO_2 and (*R,R*)-(salen-**1**)CoBr (**2.5**), (b) (*S*)-PO/CO_2 and **2.5**, (c) (*R*)-PO/CO_2 and **2.5**, (d) (*R*)-PO/CO_2 and *rac*-(salen-**1**)CoBr (**2.30**), and (e) *rac*-PO/CO_2 and **2.30**.

When (*R*)-PO is used in place of *rac*-PO, catalytic activity decreases to 50 turnovers per hour and the resultant PPC is almost perfectly regiorandom with only 43% HT connectivity (Table 2.3, entry 3; Figure 2.10c; Scheme 2.6c). In this case, degradation of the PPC to PC yields a (*S*)-PC:(*R*)-PC ratio of 34:66. Assuming PO methine attack inverts stereochemistry, while methylene attack retains stereochemistry, a HH or TT linkage in the polymer requires one (*S*)- and one (*R*)-stereocenter. Furthermore, the excess of (*R*)-PC illustrates that the HT connectivity of the parent PPC is composed of predominately (*R*)-stereocenters. This indicates that

generation of a HH linkage through misinsertion is most often immediately corrected to generate a TT linkage, followed by the incorporation of a couple of (*R*)-HT linkages until the next regioerror occurs.

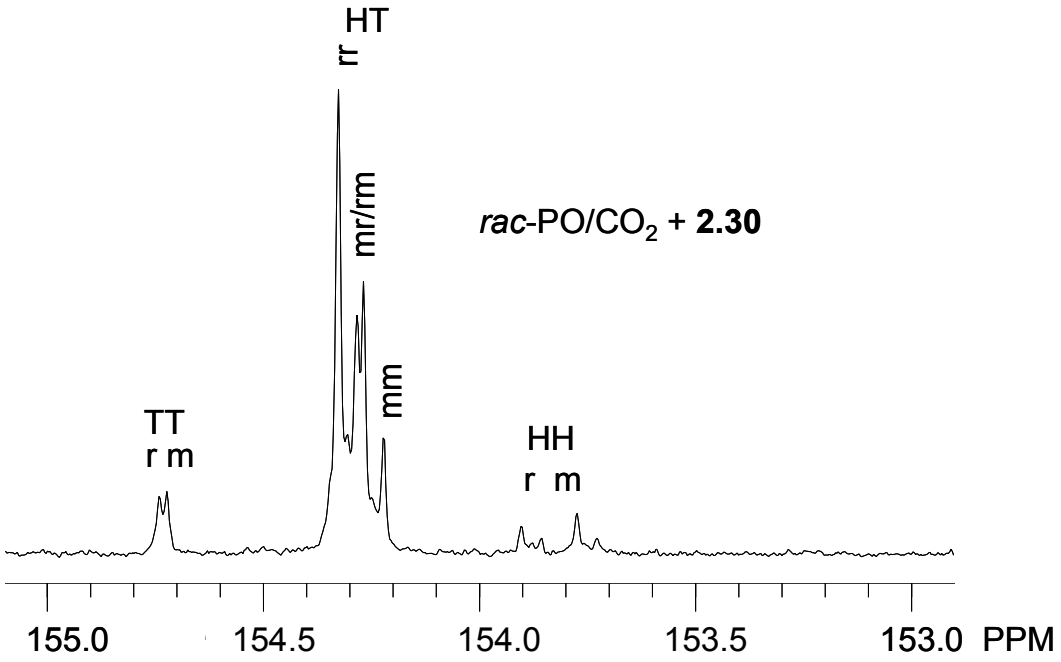

Figure 2.11. Carbonyl region of the quantitative $^{13}C\{^1H\}$ NMR ($CDCl_3$, 125 MHz, d_1 = 10s) spectrum of syndio-enriched PPC synthesized from *rac*-(salen-**1**)CoBr (**2.30**) and *rac*-PO/CO_2.

We proceeded to replace complex **2.5** with **2.30** in order to obtain further mechanistic insight concerning propagation with these systems. The copolymerization of (*R*)-PO and CO_2 with **2.30** yielded isotactic PPC with 83% HT connectivity with a catalytic activity of 100 turnovers per hour (Table 2.4, entry 4, and Scheme 2.6d). In this case, we expected two polymers with widely differing M_n values due to the predicted distinction in activity between the (*S,S*)- and (*R,R*)-catalysts with (*R*)-PO/CO_2. Interestingly, the product PPC showed a monomodal GPC trace with a MWD of 1.16, suggesting that each propagating species dissociates from the metal center during the copolymerization and is influenced by catalysts of both possible

chiralities (Scheme 2.7). The degradation PC product from this PPC has a (*S*)-PC:(*R*)-PC ratio of 9:91, again illustrating that regioerrors are immediately corrected. Finally, we investigated the *rac*-PO/CO_2 copolymerization with catalyst **2.30**. To our surprise, the product PPC, with 84% HT connectivity, has a $^{13}C\{^1H\}$ NMR spectrum unlike that of all other PPC samples (Table 2.4, entry 5, Figure 2.11, and Scheme 2.6e). In this case, the carbonyl resonances corresponding to the four HT triads ([*mm*], [*mr*], [*rm*], and [*rr*]) did not show an equal distribution. We initially assigned the most upfield HT shift in this spectrum as the [*mm*] triad (Figure 2) based on the observation that the $^{13}C\{^1H\}$ NMR HT resonance of isotactic PPC aligns with the most upfield HT resonance of atactic PPC. Furthermore, the [*mr*] and [*rm*] HT linkages should integrate equally yet show different resonances due to the directionality in the PPC. We therefore tentatively assigned the central HT resonances to the [*mr*]/[*rm*] triads and the remaining [*rr*] triad to the most downfield HT resonance, while considering that most tactic polymer systems exhibit [*mm*] and [*rr*] resonances that encompass the [*mr*]/[*rm*] $^{13}C\{^1H\}$ NMR resonances.[21, 22] Based on this scheme, we assigned the most downfield and upfield resonances in both the TT and HH portions of the spectrum to [*r*] and [*m*] diads respectfully, a simplification of the complex triad sequences from the many possible combinations of neighboring stereo- and regiosequences. It is also notable that the TT [*m*] and [*r*], HT [*m*] and [*r*], and HH [*m*] and [*r*] linkages of PPC as well as the HH [*mmm*] and [*rrr*] linkages of oligoether carbonates have been previously assigned by Chisholm and coworkers,[13, 23] and are in agreement with our PPC conformational assignments discussed above.

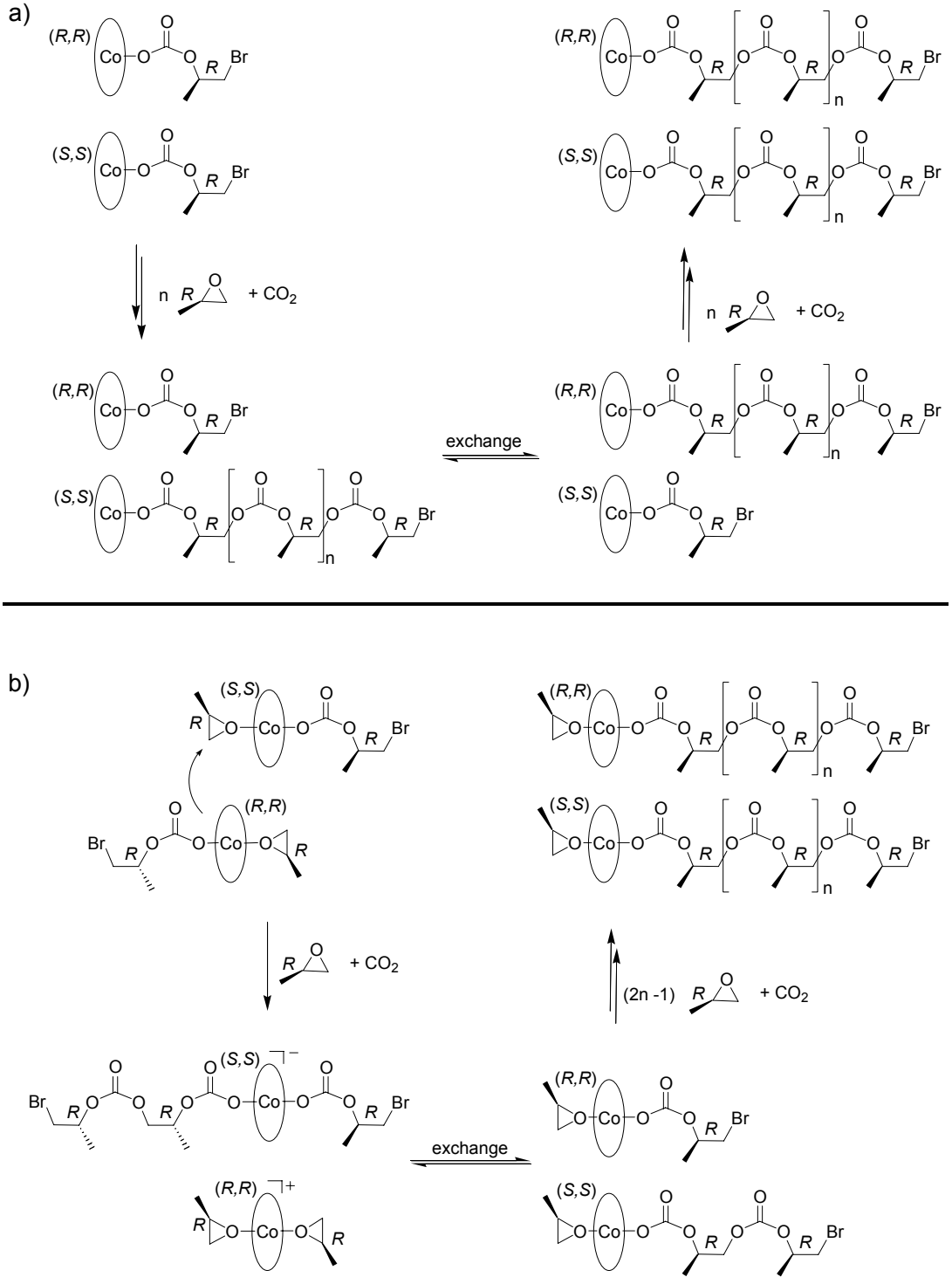

Scheme 2.7. The (*S,S*)- and (*R,R*)-(salen-**1**)CoBr catalysts a) exchange the propagating PPC in the (*R*)-PO/CO_2 copolymerization as evidenced by the isotactic PPC with a narrow MWD generated from **2.30** and (*R*)-PO/CO_2 and/or b) via a bimetallic propagation mechanism.

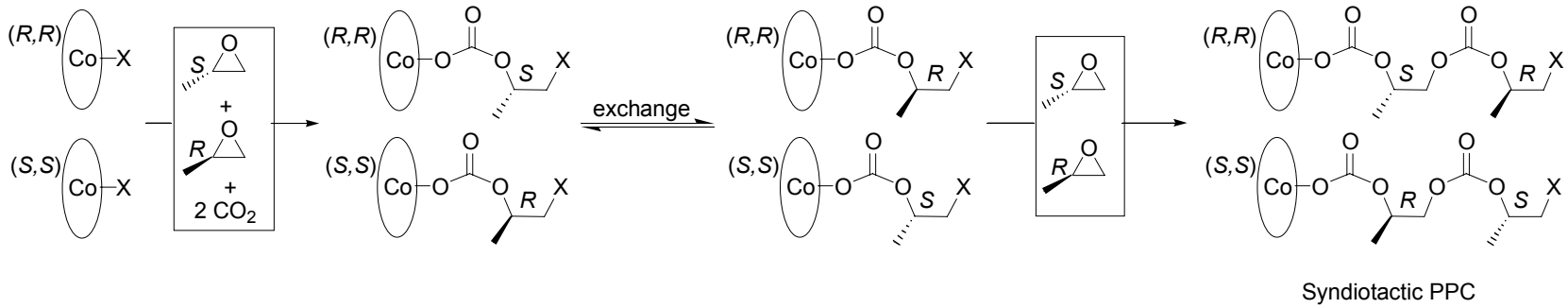

Scheme 2.8. The (*S,S*)- and (*R,R*)-(salen-**1**)CoBr catalysts exchange the propagating PPC in the *rac*-PO/CO_2 copolymerization as evidenced by the syndiotactic PPC with a narrow MWD.

Based on our $^{13}C\{^{1}H\}$ NMR assignments, the HT portion of the PPC generated from *rac*-PO/CO_2 with catalyst **2.30** is syndio-enriched, an unreported microstructure for this polymer. As the regioregularity in the PPC implicates that the PO ring-opening event occurs consistently at the less substituted carbon, we suspect that a chain-end control mechanism plays a role in the formation of syndiotactic PPC, with alternate enchainment of (*S*)- and (*R*)-PO (Scheme 2.8).[24]

Our experiments with catalysts (salen)CoX for PO/CO_2 copolymerization have led us to the following mechanistic assertions. The influence of the initiator on the copolymerization rate and the effect of combining different (salen)CoX catalysts-where a fast initiator can assist a slower one-support a bimetallic initiation similar to that proposed by Jacobsen and coworkers for the hydrolytic kinetic resolution of epoxides (Chapter 1, Scheme 1.3).[20] Additionally, the relationship of the PO and catalyst stereochemistry to the resultant PPC microstructure is consistent with a scheme in which the propagating species dissociates from the metal center during the copolymerization.

2.4 Conclusions

We have investigated a series of cobalt-based, salen-supported catalysts for the copolymerization of PO and CO_2. Through adjustment of the reaction environment and catalyst optimization we were able to maximize catalytic activity and selectivity for the generation of highly alternating, regioregular PPC with controlled molecular weight and no detectable PC. By varying catalyst and PO stereochemistry, we observed pronounced alterations in the resultant PPC microstructure, as well as changes in catalytic activity. The copolymerization of *rac*-PO/CO_2 with catalyst **2.30** yielded syndio-enriched PPC, a previously unreported microstructure for this polymer.

2.5 Experimental section

2.5.1 General procedures

All air or water sensitive reactions were carried out under dry nitrogen using an MBraun Labmaster drybox or standard Schlenk-line techniques. Methylene chloride and diethyl ether were dried and degassed by passing through a column of activated alumina and by sparging with dry nitrogen. (*S,S*)- and (*R,R*)-*N,N′*-bis(3,5-di-*tert*-butylsalicylidene)-1,2-diaminocyclohexanecobalt ((*S,S*)-(salen-**1**)Co^{II}, (*R,R*)-(salen-**1**)Co^{II}) were purchased from Aldrich and recrystallized from methylene chloride and methanol. PO was dried over calcium hydride and vacuum transferred before use. (*R*)- and (*S*)-PO were obtained using kinetic resolution as described by Jacobsen and coworkers.[25] CO_2 (99.998% purity) was purchased from Airgas and passed over a column of 4Å molecular sieves. All other reagents were purchased from commercial sources and used as received. Degradation of PPC to PC was performed according to literature procedure[10] and the product PC was analyzed by GC. Gas chromatogram were obtained on a Hewlett-Packard 6890 series gas chromatograph using a beta-DEX 225 chiral capillary column (30.0 m x 250 μm x 0.25 μm nominal), a flame ionization detector, and He carrier gas. Varian Mercury (^{1}H, 300 MHz) and Varian Inova (^{1}H, 500 MHz, $^{13}C\{^1H\}$ 125 MHz, ^{19}F 470 MHz) spectrometers were used to record $^{13}C\{^1H\}$, ^{1}H, and ^{19}F NMR spectra, which were referenced versus residual nondeuterated solvent shifts. C_6F_6 (–162.90 ppm) was used as a reference for all ^{19}F NMR spectra. Quantitative $^{13}C\{^1H\}$ ($CDCl_3$, 125 MHz, d_1 = 10s) NMR spectroscopy was used prior to integration over the carbonyl region of PPC (t_1 = 1.5s). GPC analyses were carried out using a Waters instrument (M515 pump, U6K injector) equipped with Waters UV486 and Waters 2410 differential refractive index detector, and four 5 μm PL Gel columns (Polymer Laboratories; 100 Å, 500 Å, 1000 Å, and Mixed C porosities) in series. The GPC columns were eluted with THF at 40 ºC at 1

mL/min and were calibrated using 23 monodisperse polystyrene standards. Elemental analyses were carried out by Robertson Microlit Laboratories in Madison, N.J. IR spectra were measured on a Mattson Research Series FTIR. High resolution mass spectra were obtained from the Mass Spectrometry Laboratory, School of Chemical Sciences, University of Illinois. All (salen)CoX complexes reveal axial ligand (X) loss in the (EI) mass spectra attributable to the poor stability of this complex under the applied conditions. In the case of all (salen)CoOBzF_5 complexes, carbons on the phenyl group of pentafluorobenzoate were not assigned in the $^{13}C\{^1H\}$ NMR spectra due to complex carbon fluorine splitting patterns.

2.5.2 Representative copolymerization procedure (CTC-3-251). A 100 mL Parr autoclave was heated to 120 °C under vacuum for 4 h, then cooled under vacuum to 22 °C and moved to a drybox. Complex (*R,R*)-(salen-**1**)CoOAc (19.0 mg, 0.0286 mmol), and *rac*-PO (1.00 mL, 14.3 mmol) were placed in a glass sleeve with a Teflon stir bar inside the Parr autoclave. The autoclave was pressurized to 800 psi of CO_2 and was left to stir at 22 °C for 2 h. The reactor was vented at 22 °C. A small aliquot of the resultant polymerization mixture was removed from the reactor for ^1H NMR and GPC analysis. The remaining polymerization mixture was then dissolved in methylene chloride (5 mL), quenched with 5% HCl solution in methanol (0.2 mL), and transferred to a pre-weighed vial. The product mixture was dried *in vacuo* to constant weight, and the crude yield was determined after subtracting out the catalyst weight (432 mg, 30%). The product was dissolved in methylene chloride (3 mL) and precipitated from methanol (30 mL). The polymer was collected and dried *in vacuo* to *constant* weight, and the % HT connectivity was determined using quantitative $^{13}C\{^1H\}$ NMR spectroscopy (125 MHz, $CDCl_3$, d_1 = 10s).

2.5.3 Synthesis of ligand precursors. Schiff-base condensation of salicylaldehydes with 1,2-diamines to generate salen-type ligands is readily achieved by refluxing 2

equiv of the parent aldehyde and 1 equiv of the parent diamine in absolute ethyl alcohol or THF.[26] In most cases, 3 h reaction time is sufficient for obtaining high product yields. Following the removal of solvent *in vacuo*, the crude yellow solid is recrystalized from ethyl alcohol yielding the product salen ligand in most cases. Alternatively, the HCl or tartrate salt of the parent diamine can be employed in the synthesis, where the diamine is stirred with K_2CO_3 in water until dissolution prior to reaction with the aldehyde.[27] (*R,R*)-(salen-**1**)H_2 (**2.6**) is commercially available, and can be combined in a 50:50 mixture with the commercially available (*S,S*)-(salen-**1**)H_2 to generate *rac*-(salen-**1**)H_2 (**2.7**). Alternatively, ligand **2.7** (**CTC-4-212**) can be synthesized from the Schiff-base condensation of 3,5-di-*tert*-butyl-2-hydroxybenzaldehyde with *trans*-1,2-diaminocyclohexane using the above procedure.[26] Ligands (*R*)-(salen-**2**)H_2 (**2.8, CT-1-135**),[17] (salen-**3**)H_2 (**2.9, KLP-2-77**),[28] (*R,R*)-(salen-**5**)H_2 (**2.11, KLP-2-69**),[29] (salen-**6**)H_2 (**2.12, CTC-4-210**),[30] (*R,R*)-(salen-**7**)H_2 (**2.13, CTC-3-248**),[31] (*R,R*)-(salen-**8**)H_2 (**2.14, CTC-4-110**),[16] (*R,R*)-(salen-**10**)H_2 (**2.16**, **CTC-3-196**)[32] were synthesized using the above methods[26, 27] and agree with literature characterization. The analytical data and synthetic modifications for new salen ligands are listed below:

(Salen-4)H_2 (2.10, CTC-3-151 or CTC-3-184). To a solution of 3,5-di-*tert*-butyl-2-hydroxybenzaldehyde (3.0 g, 13 mmol) in ethyl alcohol (60 mL) was added 2-methyl-1,2-propanediamine (0.67 mL, 6.4 mmol) and the mixture was refluxed for 3 h. The reaction was cooled to 22 °C, and the solvent was removed *in vacuo*. The crude yellow solid was recrystalized from ethyl alcohol at -20 °C affording yellow needles (3.1 g, 93%). ^{1}H NMR ($CDCl_3$, 500 MHz): δ 1.28 (s, 9H), 1.29 (s, 9H), 1.43 (s, 24H), 3.71 (s, 2H), 7.07 (d, ^4J = 4.5 Hz, 1H), 7.09 (d, ^4J = 4.5 Hz, 1H), 7.35 (d, ^4J = 4.5 Hz, 1H), 7.36 (d, ^4J = 4.5 Hz, 1H), 8.35 (s, 1H), 8.39 (s, 1H) 13.67 (s, 1H), 14.21 (s, 1H). ^{13}C{^{1}H} NMR ($CDCl_3$, 125 MHz): δ 25.73, 29.60, 29.63, 31.63, 31.66, 34.26, 35.17,

35.19, 60.14, 70.71, 117.99, 118.08, 126.22, 126.35, 126.90, 127.18, 136.78, 136.80, 139.98, 140.12, 158.32, 158.52, 162.88, 167.78. HRMS (ESI) *m/z* calcd ($C_{34}H_{52}N_2O_2$ + H^+) 521.4107, found 521.4110.

(*R,R*)-(Salen-9)H_2 (2.15, KLP-2-78). (*R,R*)-1,2-Diaminocyclohexane-L-tartrate (0.39 g, 1.5 mmol) and K_2CO_3 (0.40 g, 3.0 mmol) were stirred in H_2O until all was dissolved. To it was added 5-*tert*-butyl-2-hydroxybenzaldehyde (0.5 mL, 2.9 mmol) and methyl alcohol (35 mL) and the mixture was refluxed for 2.5 h. The reaction mixture was then cooled to 22 °C, and the yellow precipitate was filtered and washed with methyl alcohol. ^{1}H NMR ($CDCl_3$, 500 MHz): δ 1.24 (s, 18H), 1.47 (m, 2H), 1.71 (m, 2H), 1.89 (m, 2H), 1.94 (m, 2H), 3.29 (m, 2H), 6.83 (d, ^3J = 14 Hz, 2H), 7.12 (d, ^4J = 4.5 Hz, 2H), 7.28 (dd, ^3J = 14 Hz, ^4J = 4.5 Hz, 2H), 8.26 (s, 2H), 13.15 (s, 2H).

(*R,R*)-(Salen-11)H_2 (2.17, CTC-3-199). (*R,R*)-1,2-Diaminocyclohexane-L-tartrate (0.74 g, 2.8 mmol) and K_2CO_3 (0.77 g, 5.6 mmol) were stirred in H_2O (8 mL) until all was dissolved. To it was added a solution of 3,5-bis(α,α'-dimethylbenzyl)-2-hydroxybenzaldehyde[33] (2.0 g, 5.6 mmol) in ethyl alcohol (35 mL) and the mixture was refluxed for 3 h. The reaction mixture was then cooled to 22 °C, filtered, and washed thoroughly with H_2O and then with cold ethyl alcohol. The crude yellow solid was dried and collected (1.8 g, 81 %). ^{1}H NMR ($CDCl_3$, 500 MHz): δ 1.29 (m, 2H), 1.52 (m, 2H), 1.59 (s, 6H), 1.67 (s, 12H), 1.68 (s, 6H), 1.73 (m, 4H), 3.11 (m, 2H), 6.94 (d, ^4J = 2.5 Hz, 2H), 7.16 (tt, ^3J = 7.0 Hz, ^4J = 1.5 Hz, 2H), 7.16-7.29 (m, 20H), 8.08 (s, 2H), 13.21 (broad s, 2H). $^{13}C\{^1H\}$ NMR ($CDCl_3$, 125 MHz): δ 24.31, 28.71, 30.38, 30.95, 31.04, 33.22, 42.25, 42.44, 72.25, 118.01, 125.11, 125.68, 125.70, 126.78, 127.74, 127.92, 128.11, 129.27, 135.82, 139.46, 150.64, 150.76, 157.77, 165.38. HRMS (ESI) *m/z* calcd ($C_{56}H_{62}N_2O_2$ + H^+) 795.4890, found 795.4900.

2.5.4 Synthesis of (salen)Co^{II} precursors. All salen-ligands were metallated using cobalt acetate tetrahydrate under N_2 in a 1:1 mixture of toluene and methanol or in ethanol degassed for 20 min by sparging with dry N_2 at 22 °C for 2h or longer. Although (salen)Co^{II} complexes are generally not water-sensitive, if O_2 is present during metallation (in combination with the acetic acid generated *in situ*) most (salen)Co^{II} complexes will readily oxidize to (salen)Co^{III}OAc unless the acetic acid is removed. In most cases (salen)Co^{II} precipitates as a red or red-brown solid which can be quickly filtered in air and washed with distilled water (50 mL) and methanol (50 mL). Complex (*R,R*)-(salen-**1**)Co^{II} is commercially available and can be combined in a 50:50 mixture with the commercially available (*S,S*)-(salen-**1**)Co^{II} to generate *rac*-(salen-**1**)Co^{II}. Alternatively *rac*-(salen-**1**)Co^{II} (**CTC-4-217**) can be synthesized from ligand **2.7** using the above procedure. Complexes (salen-**3**)Co^{II} (**2.21**, **KLP-2-80**),[28] (*R,R*)-(salen-**5**)Co^{II} (**KLP-2-68**),[29] and (salen-**6**)Co^{II} (**CTC-4-216**),[30] (*R,R*)-(Salen-**7**)Co^{II} (**CTC-3-258**),[31] (*R,R*)-(salen-**8**)Co^{II} (**2.26**, **CTC-4-113**),[16] (*R,R*)-(salen-**10**)Co^{II} (**CTC-3-203**)[32] were prepared by this method are in agreement with literature reports. The analytical data and synthetic modifications for new (salen)Co complexes are listed below:

(*R*)-(Salen-2)Co^{II} (CTC-3-169). 2.3 (0.68 g, 1.3 mmol) and cobalt acetate tetrahydrate (0.40 g, 1.6 mmol) were added to a Schlenk flask charged with a Teflon stir bar under N_2. A 1:1 mixture of toluene and methanol (30 mL); (degassed for 20 min by sparging with dry N_2) was added and stirred at 22 °C for 2 h. The resultant red precipitate was filtered in air and washed with distilled water (50 mL) and methanol (50 mL) and collected as a crude red solid (0.69 g, 95%). IR (KBr, cm^{-1}): 787, 837, 874, 1179, 1204, 1255, 1320, 1361, 1385, 1466, 1528, 1596, 2871, 2909, 2956. HRMS (ESI) *m/z* calcd ($C_{33}H_{48}CoN_2O_2$) 563.3048, found 563.3046.

(Salen-4)Co^{II} (CTC-3-161). Employing the same reaction conditions as for (*R*)-(salen-**2**)Co^{II}, **2.10** (2.3 g, 4.4 mmol) and cobalt acetate tetrahydrate (1.3 g, 5.2 mmol) were used to yield the crude red solid (2.3 g, 90% yield). IR (KBr, cm^{-1}): 786, 842, 871, 1178, 1255, 1318, 1363, 1390, 1464, 1528, 1595, 2870, 2909, 2959. HRMS (ESI) *m/z* calcd ($C_{34}H_{50}CoN_2O_2$) 577.3204, found 577.3226.

(*R,R*)-(Salen-9)Co^{II} (KLP-2-86). 2.15 (0.50 g, 1.15 mmol) and cobalt acetate tetrahydrate (0.20 g, 0.8 mmol) were added to a Schlenk flask charged with a Teflon stir bar under N_2. Ethyl alcohol (30 mL); (degassed for 20 min by sparging with dry N_2) was added and stirred at 22 °C for 2 h. The resultant red precipitate was filtered in air and washed with methanol (10 mL) and collected as a crude red solid. IR (KBr, cm^{-1}): 739, 754, 816, 832, 870, 933, 1071, 1186, 1256, 1322, 1365, 1420, 1459, 1475, 1528, 1617, 2870, 2958, 3454. HRMS (ESI) m/z calcd ($C_{28}H_{36}CoN_2O_2$) 491.2109, found 491.2101.

(*R,R*)-(Salen-11)Co^{II} (CTC-3-202 or CTC-4-150). Employing the same reaction conditions as for (*R*)-(salen-**2**)Co^{II}, **2.17** (0.69 g, 0.87 mmol) and cobalt acetate tetrahydrate (0.26 g, 1.0 mmol) in a 1:1 mixture of degassed toluene and methanol (30 mL) were used to afford a crude red solid (0.59 g, 90%). IR (KBr, cm^{-1}): 766, 809, 1034, 1105, 1246, 1325, 1340, 1362, 1459, 1528, 1605, 2872, 2937, 2968, 3026, 3061, 3453. HRMS (ESI) *m/z* calcd ($C_{56}H_{60}CoN_2O_2$) 851.3987, found 851.3972.

2.5.5 Synthesis of (salen)CoX Complexes. Oxidation of (salen)Co^{II} readily occurs in the presence of a variety of acids to yield (salen)CoOAc, (salen)CoOTs (OTs = tosylate), and (salen)CoOBzF_5. Complex (salen)CoOTs can be further modified through metathesis reactions with the desired NaX salt, affording (salen)CoX (X = Cl, Br, I).[20]

(*R*,*R*)-(salen-1)CoOAc (2.1, CTC-3-140). The preparation of **2.1** has been described previously by Jacobsen and coworkers;[15] however, only 1 equiv of acetic acid was used here.

(*R*,*R*)-(Salen-1)CoCl (2.4, CTC-3-126). This complex was prepared as previously described.[20] Additional characterization: $^{13}C\{^{1}H\}$ NMR (DMSO-d_6, 125 MHz): δ 24.34, 29.51, 30.40, 31.56, 33.51, 35.78, 69.27, 118.58, 128.78, 129.28, 135.86, 141.84, 162.08, 164.68.

(*R*,*R*)-(Salen-1)CoBr (2.5, CTC-3-193 and CTC-4-146). The procedure for the synthesis of **2.4** published by Jacobsen and coworkers[20] was applied to the synthesis of complex **2.5**, with the substitution of NaBr for NaCl. ^{1}H NMR (DMSO-d_6, 500 MHz): δ 1.30 (s, 18H), 1.58 (m, 2H), 1.74 (s, 18H), 1.92 (m, 2H), 2.00 (m, 2H), 3.06 (m, 2H), 3.59 (m, 2H), 7.44 (d, ^{4}J = 3.0 Hz, 2H), 7.47 (d, ^{4}J = 3.0 Hz, 2H), 7.83 (s, 2H). $^{13}C\{^{1}H\}$ NMR (DMSO-d_6, 125 MHz): δ 24.32, 29.57, 30.43, 31.55, 33.58, 35.82, 69.32, 118.61, 128.78, 129.28, 135.87, 141.84, 162.11, 164.66. Anal. Calcd for **2.5**, $C_{36}H_{52}BrCoN_2O_2$: C, 63.25; H, 7.67; N, 4.10. Found: C, 63.05; H, 7.69; N, 4.06.

***rac*-(Salen-1)CoBr (2.30, CTC-4-220).** The procedure for the synthesis of **2.4** published by Jacobsen and coworkers[20] was applied to the synthesis of complex **2.30**, starting with *rac*-(salen-**1**)Co and with the substitution of NaBr for NaCl. (DMSO-d_6, 500 MHz) δ 1.30 (s, 18H), 1.59 (m, 2H), 1.74 (s, 18H), 1.90 (m, 2H), 2.00 (m, 2H), 3.06 (m, 2H), 3.61 (m, 2H), 7.44 (s, 2H), 7.47 (s, 2H), 7.82 (s, 2H). $^{13}C\{^{1}H\}$ NMR (DMSO-d_6, 125 MHz): δ 24.30, 29.55, 30.40, 31.48, 33.54, 35.78, 69.20, 118.59, 128.86, 129.10, 135.87, 141.79, 162.06, 164.53.

(*R*,*R*)-(Salen-1)CoI (2.2, CTC-4-6 or CTC-5-21). The procedure for the synthesis of **2.4** published by Jacobsen and coworkers[20] was applied to the synthesis of complex **2.2** with the substitution of NaI for NaCl. ^{1}H NMR (DMSO-d_6, 500 MHz): δ 1.32 (s, 18H) 1.59 (m, 2H), 1.74 (s, 18H), 1.90 (m, 2H), 2.00 (m, 2H), 3.07 (m, 2H),

3.61 (m, 2H), 7.44 (d, ^4J = 2.5 Hz, 2H), 7.47 (d, ^4J = 2.5 Hz, 2H), 7.82 (s, 2H). $^{13}C\{^1H\}$ NMR (DMSO-d_6, 125 MHz): δ 24.25, 29.59, 30.41, 30.44, 31.51, 31.58, 33.56, 35.79, 69.36, 118.61, 128.63, 128.82, 129.17, 129.37, 135.85, 141.79, 162.04, 164.51, 164.70. Anal. Calcd for $C_{36}H_{52}CoIN_2O_2$: C, 59.18; H, 7.17; N, 3.83. Found: C, 59.14; H, 7.05; N, 3.75.

Alternative procedure for (*R,R*)-(salen-1)CoI (CTC-3-63). To a solution of (*R,R*)-(salen-**1**)Co^{II} (0.6 g, 1 mmol) in dry methylene chloride (40 mL) was added iodine (0.13 g, 0.5 mmol) under N_2. The solution was stirred at 22 °C for 2.5 h and the methylene chloride was removed. The product was dissolved in dry acetonitrile, and filtered through celite under N_2 (to remove unreacted (*R,R*)-(salen-**1**)Co^{II} the acetonitrile was removed and the product was suspended in dry pentane and filtered. The solid was dried in vacuo to yield the product (*R,R*)-(salen-**1**)CoI. ^1H NMR (DMSO-d_6, 500 MHz): δ 1.32 (s, 18H) 1.59 (m, 2H), 1.74 (s, 18H), 1.90 (m, 2H), 2.01 (m, 2H), 3.07 (m, 2H), 3.60 (m, 2H), 7.44 (d, ^4J = 2.5 Hz, 2H), 7.47 (d, ^4J = 2.5 Hz, 2H), 7.82 (s, 2H). $^{13}C\{^1H\}$ NMR (DMSO-d_6, 125 MHz): δ 24.31, 29.56, 30.37, 30.41, 31.47, 31.54, 33.53, 35.77, 69.25, 118.56, 128.64, 128.82, 129.11, 129.31, 135.85, 141.77, 162.02, 164.49, 164.66.

(*R,R*)-(Salen-1)CoOBzF$_5$ (2.3, CTC-4-90 or CTC-4-193). (*R,R*)-(Salen-**1**)Co^{II} (1.2 g, 2.0 mmol) and pentafluorobenzoic acid (0.4 g, 2.0 mmol) were added to a 50 mL round-bottomed flask charged with a Teflon stir bar. Toluene (20 mL) was added to the reaction mixture, and it was stirred open to air at 22 °C for 12 h. The solvent was removed by rotary evaporation at 22 °C, and the solid was suspended in 200 mL of pentane and filtered. The dark green crude material was dried *in vacuo* and collected in quantitative yield. ^1H NMR (DMSO-d_6, 500 MHz): δ 1.30 (s, 18H), 1.59 (m, 2H), 1.74 (s, 18H), 1.90 (m, 2H), 2.00 (m, 2H), 3.07 (m, 2H), 3.60 (m, 2H), 7.44 (d, ^4J = 2.5 Hz, 2H), 7.47 (d, ^4J = 3.0 Hz, 2H), 7.81 (s, 2H). $^{13}C\{^1H\}$ NMR (DMSO-d_6,

125 MHz): δ 24.39, 29.61, 30.13, 30.42, 31.55, 33.57, 35.83, 69.38, 118.59, 128.78, 129.29, 135.86, 141.83, 162.21, 164.66. ^{19}F NMR (470 MHz, DMSO-d_6): ∂ –163.32 (m), –162.50 (m), –144.48 (m). Anal. Calcd for $C_{43}H_{52}CoF_5N_2O_4 \cdot H_2O$: C, 62.01; H, 6.54; N, 3.36. Found: C, 62.25; H, 6.38; N, 3.42.

(*R*)-(Salen-2)CoBr (2.18, CTC-3-174). (*R*)-(Salen-**2**)Co^{II} (0.50 g, 0.89 mmol) and *p*-toluenesulfonic acid monohydrate (0.18 g, 0.94 mmol) were added to a 50 mL round-bottomed flask charged with a Teflon stir bar. Methylene chloride (10 mL) was added to the reaction mixture and stirred for 1 h open to air at 22 °C. The solvent was removed by rotary evaporation at 22 °C, and the dark green solid was dissolved in pentane and filtered. The solvent was removed by rotary evaporation, and the material was dissolved in methylene chloride (50 mL) and added to a 250 mL separatory funnel. The organic layer was shaken vigorously with saturated aqueous NaBr (3 x 50 mL). The organic layer was dried over Na_2SO_4 and evaporated under reduced pressure to afford a crude black solid (0.29 g, 50%). ^{1}H NMR (DMSO-d_6, 500 MHz): δ 1.298 (s, 9H), 1.303 (s, 9H) 1.61 (d, ^3J = 7.0 Hz, 3H), 1.727 (s, 9H), 1.736 (s, 9H), 3.86 (m, 1H), 4.21 (m, 1H), 4.32 (m, 1H), 7.33 (d, ^4J = 2.5 Hz, 1H), 7.40 (d, ^4J = 2.5 Hz, 1H), 7.44 (d, ^4J = 2.5 Hz, 1H), 7.45 (d, ^4J = 2.5 Hz, 1H), 7.93 (s, 1H), 8.09 (s, 1H). ^{13}C{^{1}H} NMR (DMSO-d_6, 125 MHz): δ 18.51, 30.38, 30.41, 31.57, 33.47, 35.77, 63.03, 64.61, 118.58, 118.89, 128.22, 128.72, 135.84, 136.00, 141.76, 142.04, 161.73, 162.01, 167.10, 168.63.

(Salen-3)CoBr (2.20, CTC-3-187). Employing the same reaction conditions as for **2.18**, **2.21** (0.30 g, 0.55 mmol) and *p*-toluenesulfonic acid monohydrate (0.10 g, 0.55 mmol) were used. Following the salt metathesis with NaBr, the crude product **2.20** was obtained (86 mg, 25%). ^{1}H NMR (DMSO-d_6, 500 MHz): δ 1.30 (s, 18H), 1.73 (s, 18H), 4.14 (s, 4H), 7.31 (d, ^4J = 3.0 Hz, 2H), 7.45 (d, ^4J = 3.0 Hz, 2H), 8.12

(s, 2H). $^{13}C\{^{1}H\}$ NMR (DMSO-d_6, 125 MHz): δ 30.36, 31.52, 33.43, 35.77, 58.24, 118.51, 128.27, 128.74, 135.93, 142.05, 162.13, 168.65.

(Salen-4)CoBr (2.19, CTC-3-168 or CTC-3-264). Employing the same reaction conditions as for **2.18**, (salen-**4**)Co^{II} (0.30 g, 0.52 mmol) and *p*-toluenesulfonic acid monohydrate (99 mg, 0.52 mmol) were used. Following the salt metathesis with NaBr, the crude product **2.19** was obtained (92 mg, 27%). ^{1}H NMR (DMSO-d_6, 500 MHz): δ 1.30 (s, 9H), 1.32 (s, 9H), 1.63 (s, 6H), 1.73 (s, 9H), 1.74 (s, 9H), 4.02 (s, 2H), 7.36 (d, ^{4}J = 2.5 Hz, 1H), 7.45 (d, ^{4}J = 2.5 Hz, 1H), 7.475 (s, 1H), 7.482 (s, 1H), 7.88 (s, 1H), 8.03 (s, 1H). $^{13}C\{^{1}H\}$ NMR (DMSO-d_6, 125 MHz): δ 27.10, 30.35, 31.28, 31.32, 31.55, 31.61, 33.43, 33.50, 35.72, 35.77, 66.98, 70.93, 118.36, 119.57, 128.05, 128.75, 128.98, 129.35, 135.85, 136.41, 141.42, 142.12, 161.11, 161.96, 166.31, 168.37. HRMS (EI) *m/z* calcd ($C_{34}H_{50}BrCoN_2O_2$ – Br) 577.3204, found 577.3199.

(*R,R*)-(Salen-5)CoBr (2.22, CTC-3-166). (*R,R*)-(Salen-**5**)Co^{II} (0.25 g, 0.36 mmol) and *p*-toluenesulfonic acid monohydrate (68 mg, 0.36 mmol) were added to a 50 mL round bottomed flask charged with a Teflon stir bar. Methylene chloride (10 mL) was added to the reaction mixture and stirred for 2 h open to air at 22 °C. The solvent was removed by rotary evaporation at 22 °C, and the crude solid was washed with pentane (100 mL) and filtered. The crude material was dissolved in methylene chloride (25 mL) and added to a 125 mL separatory funnel. The organic layer was rinsed with saturated aqueous NaBr (3 x 25 mL). The organic layer was dried over Na_2SO_4 and evaporated under reduced pressure. The solid was washed with pentane (100 mL) and filtered to afford **2.22** (0.12 g, 43%). ^{1}H NMR (DMSO-d_6, 500 MHz): δ 1.22 (s, 18H), 1.76 (s, 18H), 5.62 (s, 2H), 6.97 (s, 2H), 7.23 (s, 2H), 7.41- 7.48 (m, 12H). $^{13}C\{^{1}H\}$ NMR (DMSO-d_6, 125 MHz): δ 30.37, 31.35, 33.31, 35.73, 76.61,

117.64, 128.48, 129.18, 129.90, 134.93, 136.07, 142.02, 162.31, 166.50. HRMS (EI) *m/z* calcd. ($C_{44}H_{54}BrCoN_2O_2$ – Br) 701.3517 found 701.3502.

(Salen-6)CoBr (2.23, CTC-4-221). Employing the same reaction conditions as for **2.22**, (salen-**6**)Co^{II} (1.0 g, 1.7 mmol) and *p*-toluenesulfonic acid monohydrate (0.32 g, 1.7 mmol) were used to produce **2.23** (0.35 g, 30%). ^{1}H NMR (DMSO-d_6, 500 MHz): δ 1.35 (s, 18H), 1.78 (s, 18H), 7.55 (d, ^4J = 2.5 Hz, 2H), 7.56 (td, ^3J = 6.5 Hz, ^4J = 3.5 Hz, 2H), 7.66 (d, ^4J = 2.5 Hz, 2H), 8.63 (dd, ^3J = 6.5 Hz, ^4J = 3.5 Hz, 2H), 8.95 (s, 2H). ^{13}C{^{1}H} NMR (DMSO-d_6, 125 MHz): δ 30.34, 31.34, 33.79, 36.01, 117.40, 117.45, 128.14, 129.97, 131.00, 136.59, 142.07, 144.72, 161.60, 165.59. HRMS (EI) *m/z* calcd ($C_{36}H_{46}BrCoN_2O_2$ – Br) 597.2891, found 597.2878.

(*R,R*)-(Salen-7)CoBr (2.24, CTC-3-173). Employing the same reaction conditions as for **2.22**, (*R,R*)-(salen-**7**)Co^{II} (470 mg, 0.96 mmol) and *p*-toluenesulfonic acid monohydrate (190 mg, 1.0 mmol) were used to produce **2.24** (210 mg, 38%). ^{1}H NMR (DMSO-d_6, 500 MHz): δ 1.59 (m, 2H), 1.73 (s, 18H), 1.90 (m, 2H), 2.01 (m, 2H), 3.06 (m, 2H), 3.60 (m, 2H), 6.59 (t, ^3J = 7.0 Hz, 2H), 7.38 (d, ^3J = 7.0 Hz, 2H), 7.49 (d, ^3J = 7.0 Hz, 2H), 7.87 (s, 2H). ^{13}C{^{1}H} NMR (DMSO-d_6, 125 MHz): δ 24.18, 29.49, 30.31, 35.62, 69.33, 114.47, 119.19, 131.17, 133.83, 142.49, 164.19, 164.37.

(*R,R*)-(Salen-8)CoBr (2.25, CTC-3-208). Employing the same reaction conditions as for **2.22**, **2.26** (360 mg, 0.56 mmol) and *p*-toluenesulfonic acid monohydrate (110 mg, 0.60 mmol) were stirred for 12 h in methylene chloride (10 mL). Following the salt metathesis with NaBr, the product **2.25** was obtained (180 mg, 44%). ^{1}H NMR (DMSO-d_6, 500 MHz): δ 1.59 (m, 2H), 1.71 (s, 18H), 1.88 (m, 2H), 2.00 (m, 2H), 3.04 (m, 2H), 3.61 (m, 2H), 7.37 (d, ^4J = 2.5 Hz, 2H), 7.80 (d, ^4J = 2.5 Hz, 2H), 7.96 (s, 2H). ^{13}C{^{1}H} NMR (DMSO-d_6, 125 MHz): δ 24.06, 29.51, 29.85, 35.78, 69.55, 104.97, 120.73, 133.45, 135.04, 145.16, 163.19, 164.22.

(*R,R*)-(Salen-9)CoBr (2.27, CTC-3-207). The procedure for the synthesis of **2.22** was applied to the synthesis of **2.27**, using (*R,R*)-(salen-**9**)Co^{II} (220 mg, 0.45 mmol) and *p*-toluenesulfonic acid monohydrate (89 mg, 0.47 mmol). Following the salt metathesis with NaBr, the product **2.27** was obtained (94 mg, 37%). ^{1}H NMR (DMSO-d_6, 500 MHz): δ 1.29 (s, 18H), 1.56 (m, 2H), 1.85 (m, 2H), 2.00 (m, 2H), 3.05 (m, 2H), 3.57 (m, 2H), 7.39 (d, ^{3}J = 8.5 Hz, 2H), 7.46 (dd, ^{3}J = 8.5 Hz, ^{4}J = 2.5 Hz, 2H), 7.61 (d, ^{4}J = 2.5 Hz, 2H), 8.02 (s, 2H). $^{13}C\{^{1}H\}$ NMR (DMSO-d_6, 125 MHz): δ 24.20, 29.52, 31.38, 33.47, 69.46, 117.96, 122.18, 130.92, 132.46, 137.00, 163.04, 164.32.

(*R,R*)-(Salen-10)CoBr (2.28, CTC-3-211). The procedure for the synthesis of **2.22** was applied to the synthesis of **2.28**, however, (*R,R*)-(salen-**10**)Co^{II} (210 mg, 0.52 mmol) and *p*-toluenesulfonic acid monohydrate (100 mg, 0.53 mmol) were stirred for 2 h in methylene chloride (20 mL). An excess of methylene chloride (200 mL) was used in the salt metathesis with NaBr in order to dissolve all of the (*R,R*)-(salen-**10**)CoOTs intermediate. Following this reaction, the product **2.28** was obtained (170 mg, 67%). ^{1}H NMR (DMSO-d_6, 500 MHz): δ 1.57 (m, 2H), 1.86 (m, 2H), 1.99 (m, 2H), 2.64 (s, 6H), 3.05 (m, 2H), 3.63 (m, 2H), 6.58 (t, ^{3}J = 7.0 Hz, 2H), 7.31 (d, ^{3}J = 7.0 Hz, 2H), 7.48 (d, ^{3}J = 7.0 Hz, 2H), 8.02 (s, 2H). $^{13}C\{^{1}H\}$ NMR (DMSO-d_6, 125 MHz): δ 17.12, 24.17, 29.45, 69.60, 114.57, 117.89, 130.68, 132.86, 134.36, 163.32, 164.13.

(*R,R*)-(Salen-11)CoBr (2.29, CTC-3-241). Employing the same reaction conditions as for **2.22**, (*R,R*)-(salen-**11**)Co^{II} (0.50 g, 0.59 mmol) and *p*-toluenesulfonic acid monohydrate (0.11 g, 0.59 mmol) were stirred for 5 h to afford the crude black solid **2.29** (0.16 g, 29%).[b] ^{1}H NMR (DMSO-d_6, 500 MHz): δ 1.50 (m, 2H), 1.57 (s,

[b] To remove trace amounts of paramagnetic (salen)Co^{II} to obtain NMR spectra, the product was dissolved in acetonitrile and filtered through celite and then the acetonitrile was removed prior to dissolution in DMSO-d_6.

6H), 1.58 (s, 6H), 1.76 (s, 6H), 1.84 (m, 2H), 1.93 (m, 2H), 2.29 (s, 6H), 2.92 (m, 2H), 3.39 (m, 2H), 6.98 (d, ^{4}J = 3.0 Hz, 2H), 7.06 (tt, ^{3}J = 9.0 Hz, ^{4}J = 2.0 Hz, 2H), 7.12 – 7.28 (m, 18H), 7.45 (d, ^{4}J = 2.5 Hz, 2H), 7.75 (s, 2H). $^{13}C\{^{1}H\}$ NMR (DMSO-d_6, 125 MHz): δ 24.19, 27.92, 27.98, 29.56, 30.31, 30.42, 30.51, 30.54, 32.55, 41.43, 41.57, 41.90, 43.36, 69.07, 118.92, 125.09, 125.35, 125.39, 125.52, 126.17, 126.20, 126.37, 127.66, 127.74, 127.88, 127.94, 130.80, 133.02, 135.11, 135.14, 141.02, 150.72, 151.20, 161.90, 164.70.

2.6 References

(1) (a) Arakawa, H. *et al. Chem. Rev.* **2001**, *101*, 953-996. (b) Musie, G.; Wei, M.; Subramaniam, B.; Busch, D. H. *Coord. Chem. Rev.* **2001**, *219*, 789-820. (c) Cooper, A. I. *J. Mater. Chem.* **2000**, *10*, 207-234. (d) Bolm, C.; Beckmann, O.; Dabard, O. A. G. *Angew. Chem. Int. Ed.* **1999**, *38*, 907-909. (e) Yin, X. L.; Moss, J. R. *Coord. Chem. Rev.* **1999**, *181*, 27-59. (f) Gibson, D. H. *Chem. Rev.* **1996**, *96*, 2063-2095. (g) Leitner, W. *Coord. Chem. Rev.* **1996**, *153*, 257-284. (h) Leitner, W. *Angew. Chem. Int. Ed.* **1995**, *34*, 2207-2221. (i) Jessop, P. G.; Ikariya, T.; Noyori, R. *Chem. Rev.* **1995**, *95*, 259-272.

(2) For reviews on epoxide/CO_2 copolymerizations, see: (a) Ochiai, B.; Endo, T. *Prog. Polym. Sci.* **2005**, *30*, 183 - 215. (b) Moore; D. R.; Coates, G. W. *Angew. Chem. Int. Ed.* **2004**, *43*, 6618 - 6639. (c) Sugimoto H.; Inoue S. *J. Polym. Sci. Polym. Chem.* **2004**, *42*, 5561 - 5573. (d) Darensbourg, D. J.; Mackiewicz, R. M.; Phelps, A. L.; Billodeaux, D. R. *Acc. Chem. Res.* **2004**, *37*, 836 - 844. (e) Darensbourg, D. J.; Holtcamp, M. W. *Coord. Chem. Rev.* **1996**, *153*, 155 - 174. (f) Super, M. S.; Beckman, E. J. *Trends Polym. Sci.* **1997**, *5*, 236 - 240. (g) Kuran, W. *Prog. Polym. Sci.* **1998**, *23*, 919 - 992. (h) Aida, T.; Inoue, S. *Acc. Chem. Res.* **1996**, *29*, 39 - 48.

(3) (a) Inoue, S.; Koinuma H.; Tsuruta, T. *J. Polym. Sci. Polym. Phys.* **1969**, *7*, 287 - 292. (b) Inoue, S.; Koinuma, H.; Tsuruta, T. *Makromol. Chem.* **1969**, *130*, 210 - 220.

(4) Darensbourg, D. J.; Yarbrough, J. C.; Ortiz, C.; Fang, C. C. *J. Am. Chem. Soc.* **2003**, *125*, 7586-7591.

(5) Allen, S. D.; Moore, D. R.; Lobkovsky, E. B.; Coates, G. W. *J. Am. Chem. Soc.* **2002**, *124*, 14284-14285.

(6) Eberhardt, R.; Allmendinger, M.; Rieger, B. *Macromol. Rapid Commun.* **2003**, *24*, 194-196.

(7) Ree, M.; Bae, J. Y.; Jung, J. H.; Shin, T. J. *J. Polym. Sci. Polym. Chem.* **1999**, *37*, 1863-1876.

(8) Aida, T.; Ishikawa, M.; Inoue, S. *Macromolecules* **1986**, *19*, 8-13.

(9) Darensbourg, D. J.; Yarbrough, J. C. *J. Am. Chem. Soc.* **2002**, *124*, 6335-6342.

(10) Chisholm, M. H.; Navarro-Llobet, D.; Zhou, Z. P. *Macromolecules* **2002**, *35*, 6494-6504.

(11) Darensbourg, D. J.; Phelps, A. L. *Inorg. Chem.* **2005**, *44*, 4622-4629.

(12) Darensbourg, D. J.; Mackiewicz, R. M.; Rodgers, J. L.; Phelps, A. L. *Inorg. Chem.* **2004**, *43*, 1831-1833.

(13) Chisholm, M. H.; Zhou, Z. P. *J. Am. Chem. Soc.* **2004**, *126*, 11030-11039.

(14) Coates, G. W. *Chem. Rev.* **2000**, *100*, 1223-1252.

(15) Tokunaga, M.; Larrow, J. F.; Kakiuchi, F.; Jacobsen, E. N. *Science* **1997**, *277*, 936-938.

(16) Qin, Z.; Thomas, C. M.; Lee, S.; Coates, G. W. *Angew. Chem. Int. Ed.* **2003**, *42*, 5484-5487.

(17) Darensbourg, D. J.; Mackiewicz, R. M.; Rodgers, J. L.; Fang, C. C.; Billodeaux, D. R.; Reibenspies, J. H. *Inorg. Chem.* **2004**, *43*, 6024-6034.

(18) Darensbourg, D. J.; Mackiewicz, R. M.; Billodeaux, D. R. *Organometallics* **2005**, *24*, 144-148.

(19) Inoue, S. *J. Polym. Sci. Polym. Chem.* **2000**, *38*, 2861-2871.

(20) Nielsen, L. P. C.; Stevenson, C. P.; Blackmond, D. G.; Jacobsen, E. N. *J. Am. Chem. Soc.* **2004**, *126*, 1360-1362.

(21) Resconi, L.; Cavallo, L.; Fait, A.; Piemontesi, F. *Chem. Rev.* **2000**, *100*, 1253-1345.

(22) Schilling, F. C.; Tonelli, A. E. *Macromolecules* **1986**, *19*, 1337-1343.

(23) Byrnes, M. J.; Chisholm, M. H.; Hadad, C. M.; Zhou, Z. P. *Macromolecules* **2004**, *37*, 4139-4145.

(24) Ovitt, T. M.; Geoffrey, W. C. *J. Am. Chem. Soc.* **2002**, *124*, 1316-1326.

(25) Schaus, S. E.; Brandes, B. D.; Larrow, J. F.; Tokunaga, M.; Hansen, K. B.; Gould, A. E.; Furrow, M. E.; Jacobsen, E. N. *J. Am. Chem. Soc.* **2002**, *124*, 1307-1315.

(26) Zhang, W.; Jacobsen, E. N. *J. Org. Chem.* **1991**, *56*, 2296-2298.

(27) Pospisil, P. J.; Carsten, D. H.; Jacobsen, E. N. *Chem. Eur. J.* **1996**, *2*, 974-980.

(28) Rhodes, B.; Rowling, S.; Tidswell, P.; Woodward, S.; Brown, S. M. *J. Mol. Catal. A.* **1997**, *116*, 375-384.

(29) Fukuda, T.; Katsuki, T. *Tetrahedron* **1997**, *53*, 7201-7208.

(30) Shimakoshi, H.; Takemoto, H.; Aritome, I.; Hisaeda, Y. *Tetrahedron Lett.* **2002**, *43*, 4809-4812.

(31) Sun, W.; Xia, C.-G.; Zhao, P.-Q. *J. Mol. Catal. A* **2002**, *184*, 51-55.

(32) Szlyk, E.; Surdykowski, A.; Barwiolek, M.; Larsen, E. *Polyhedron* **2002**, *21*, 2711-2717.

(33) Cherian, A. E.; Lobkovsky, E. B.; Coates, G. W. *Macromolecules* **2005**, *38*, 6259-6268.